RESEARCH ARTICLE

Macromolecular Materials and Engineering
Open Access
www.mame-journal.de

Selective Functionalization of MWCNTs: Enhancing Wear Mechanisms and Friction-Induced Graphitization in Epoxy Composites

*Ravisrini Jayasinghe, Maximiano Ramos, Ashveen Nand, and Maziar Ramezani**

This investigation elucidates a novel methodology for augmenting the tribological and mechanical attributes of epoxy composites via selective functionalization of multi-walled carbon nanotubes (MWCNTs). The study optimizes wear mechanisms and friction-induced graphitization by incorporating pristine (P-MWCNTs), carboxyl-functionalized (COOH-MWCNTs), amine-functionalized (NH_2-MWCNTs), and silane-modified MWCNTs. Composites were characterized for tensile strength, compressive strength, surface hardness, coefficient of friction (COF), and specific wear rate (SWR). Incorporation of 0.3 wt.% COOH-MWCNTs yielded optimal performance, reducing SWR by 82% (0.07×10^{-6} mm^3 $N^{-1}{\cdot}m^{-1}$ at 8 Hz) and COF by 32% (0.37 at 10 N) relative to neat epoxy (SWR: 0.50×10^{-6} mm^3 $N^{-1}{\cdot}m^{-1}$, COF: 0.66 at 15 N). Enhanced dispersion, interfacial adhesion, and tribofilm formation account for superior tensile strength (≈90 MPa) and hardness (≈88 Shore D). X-ray diffraction and transmission electron microscopy validated friction-induced graphitization and partial structural degradation above 10 N. Applications encompass self-lubricating bushings, protective coatings, and wear-resistant surfaces for automotive and industrial components. Future investigations should target enhanced compressive strength and load-bearing capacity.

1. Introduction

Many researchers have reported promising results from carbon-based fillers in epoxy composites. Incorporating carbon nanofillers like single-walled carbon nanotubes SWCNT, multi-walled carbon nanotubes (MWCNT), Carbon nanofibers (CNFs), graphene, and Carbon black (CB) into an epoxy matrix can enhance the structural and functional properties of polymer-based composites, including mechanical and electrical conductivity.[1,2] The addition of MWCNTs to epoxy composites has been demonstrated to significantly improve their mechanical properties, including tensile strength, toughness, and modulus. MWCNTs have excellent mechanical properties, including high tensile strength, stiffness, and aspect ratio, making them ideal for reinforcing epoxy matrices. However, the effectiveness of MWCNTs in improving epoxy's mechanical characteristics is determined by how well they disperse inside the matrix and interact at the interface.[3] Functionalization of MWCNTs has emerged as a critical technique for improving their compatibility and interfacial interaction with the epoxy matrix. Functional groups such as carboxyl (-COOH) or amine (-NH_2) can be grafted onto MWCNT surfaces to increase their dispersion in epoxy and facilitate chemical interaction between the nanotubes and the polymer. This results in more effective load transfer from the matrix to the nanotubes, which enhances mechanical performance.[4,5]

The functionalization of MWCNTs has emerged as a key method for improving the mechanical properties of epoxy composites. This experiment explores the impact of different functionalization techniques, such as carboxyl (COOH), amine (NH_2), and coupling agents, on the wear mechanisms within epoxy composites. Carbon nanotubes (CNTs), since their discovery in 1991, have been of great interest due to their remarkable properties, including high tensile strength, thermal conductivity, and electrical performance.[6] Specifically, MWCNTs, which consist of multiple concentric graphene layers, offer significant advantages when incorporated into polymer matrices like epoxy resins.[7] However, the inherent hydrophobicity and poor dispersion of P-MWCNTs in polymer matrix have hindered their full potential in composites. Functionalization, whether covalent or non-covalent, is an effective method for enhancing the interfa-

R. Jayasinghe, M. Ramos, M. Ramezani
Department of Mechanical Engineering
Auckland University of Technology
Auckland 1010, New Zealand
E-mail: maziar.ramezani@flinders.edu.au

A. Nand
Faculty of Engineering
University of Auckland
Auckland 1010, New Zealand

M. Ramezani
College of Science and Engineering
Flinders University
Adelaide 5042, Australia

The ORCID identification number(s) for the author(s) of this article can be found under https://doi.org/10.1002/mame.202500088

DOI: 10.1002/mame.202500088

cial interaction between MWCNTs and the epoxy matrix, resulting in improved load transmission and wear resistance.[8,9] P-MWCNTs are known to improve the tensile and flexural characteristics of composites by strengthening the matrix. However, the poor interfacial contact between unmodified MWCNTs and the epoxy matrix frequently restricts their efficacy in enhancing wear characteristics.[10] Wear mechanisms in such composites often include abrasive wear, with agglomerate clusters of MWCNTs acting as abrasive particles themselves, resulting in increased wear debris.[11]

Incorporating MWCNTs into epoxy composites improves tribological performance. Mucha et al.[12] found that MWCNT content between 0.25 and 0.5 wt.% achieved optimal wear resistance in epoxy resin for aerospace applications. Cui et al.[13] demonstrated that increasing MWCNT loading from 0 to 0.5 wt.% reduced wear rate, with 0.5 wt.% amino-MWCNTs achieving a 41.3% reduction. The lowest COF (0.28) was obtained with 0.1 wt.% acid-functionalized MWCNTs. Kurien et al.[14] reported that 0.5 wt.% MWCNTs provided the best tribological performance, exhibiting minimal abrasive wear and excellent filler bonding. Campo et al[15] found that 0.5 wt.% of NH_2-NMWCNT (short fibers) dispersed by calendering displayed the best tribological properties among the various types and percentages tested. These findings support the selection of 0.1–0.5 wt.% MWCNTs for enhancing epoxy composite performance. These findings support the selection of 0.1–0.5 wt.% MWCNTs for enhancing epoxy composite performance. Cui et al.[13] investigated the effect of surface modification, MWCNT content, applied load, and sliding speed on the friction and wear performance of MWCNT/epoxy composites at MWCNT loadings of 0, 0.1, 0.3, and 0.5 wt.%. A steel ring was rotated against epoxy composites filled with P-MWCNTs, acid-functionalized MWCNTs (COOH-MWCNTs), and amino-functionalized MWCNTs NH_2-MWCNTs for 40 min under applied loads of 40, 80, and 120N. Wear rates for 0.5 wt.% P-MWCNT, COOH-MWCNT, and NH_2-MWCNT/epoxy composites were 1.149×10^{-4}, 1.001×10^{-4}, and 0.953×10^{-4} g min^{-1}, respectively. These composites showed 22.2%, 38.3%, and 41.3% wear rate reductions compared to clean epoxy, illustrating the efficacy of MWCNT inclusion, particularly with functionalized CNTs, in improving wear resistance. The 0.5 wt.% NH_2-MWCNT composite has the lowest wear rate, down 41.3% compared to pure epoxy. The strong association between functionalized MWCNTs and epoxy reduces localised stress concentrations and increases thermal resistance.[] Overall, these advances render MWCNT-epoxy composites ideal for demanding industrial applications.[16,17]

Barrena et al.[18] investigated the effect of filler content on the wear resistance of CNF/epoxy nanocomposites. Wear experiments were performed using a ball-on-disk tribometer, in which an epoxy/CNF nanocomposite disc was rubbed against a C-Cr steel ball at sliding distances ranging from 500 to 2000m, at a sliding speed of 0.2m s^{-1} under 5N stress. They found that, while untreated CNFs can minimize mass and wear volume loss in epoxy resin, the friction coefficient increases partially when the CNF level approaches 2 wt.%. Further, they have concluded that surface modification of CNFs by oxidative treatment introduces carboxyl groups, which improves the interface between the reinforcement and the matrix as well as filler dispersion. This treatment resulted in a 30% to 40% increase in wear resistance over the untreated CNF composite. Adhesion is the primary wear mechanism in unfilled epoxy, although adding CNF fillers reduces adhesive wear while increasing abrasive wear. However, functionalized CNFs used in composite manufacturing greatly reduce abrasive wear.[18] The addition of carboxyl groups strengthens the chemical interaction between the nanotubes and the epoxy matrix, resulting in improved dispersion and stress transfer.[19]

Lee et al.[20] studied the wear properties of epoxy composites containing oxidized MWCNTs and silane-treated MWCNTs (3-aminopropyltriethoxysilane). A zirconia ball was employed as the counter material, and wear tests were carried out utilizing the pin-on-disc method. The experiments were carried out at three sliding speeds (0.12, 0.18, and 0.24 m s^{-1}) over a set sliding distance of 2750m with a load of 10N. At the slowest sliding speed (0.12 m s^{-1}), both composites had comparable friction coefficients ranging from 0.13 to 0.22. However, as the sliding speed increased to 0.18 and 0.24 m s^{-1}, the friction coefficients of both composites rose dramatically (0.55 to 0.65). Despite this, silanized CNT/epoxy nanocomposites consistently demonstrated lower friction coefficients than oxidized CNT/epoxy composites at all speeds. At normal sliding speeds, both composites suffered exfoliation, although the silanized composites showed much less material peeling. At higher sliding speeds, both materials developed massive cracks and wear marks, however the level of damage was much decreased in the silanized samples. They conclude that silanization procedure provides improved dispersion and stronger interfacial adhesion between CNTs and the epoxy matrix, which accounts for this improvement.[20] The strong connection between the silane-treated fillers and the epoxy matrix reduces the possibility of stress concentrations or delamination, contributing to increased toughness and resistance to mechanical failure.[21] Furthermore, silane-modified fillers exhibit improved dispersion inside the epoxy matrix. This enhanced compatibility guarantees a consistent dispersion of reinforcing particles, avoiding the creation of weak areas that may cause failure under mechanical loads. The silane agent's chemical interaction improves the composite's resilience to moisture and environmental deterioration, leading to greater epoxy durability under hard environments. Overall, silane coupling agents improve epoxy composites' mechanical performance, durability, and long-term stability, making them suitable for usage in automotive, aerospace, and structural applications.[22,23]

Pincheira et al.[24] investigated the influence of amino-functionalized multiwall carbon nanotubes on the dry sliding wear resistance of carbon fiber reinforced thermoset polymers. MWCNTs were found to improve both compression strength and specific wear rate; it is determined that MWCNTs also affect matrix/reinforcement interfacial strength and matrix fracture toughness. However, the dry-sliding tribology tests revealed that the incorporation of MWCNTs in the composite did not change the friction coefficient but tended to minimize the specific wear rate. However, details about how this happens were not provided. Liu et al.[25] investigated the effects of poly(ethyleneimine) functionalized multi-walled carbon nanotubes on the mechanical and tribological properties of epoxy resin. The wear test was performed on specimens using a friction tester with a normal

load of 100 N, rotation speed of 150 r min^{-1}, and a test period of 30 min. Using 0.7wt% poly(ethyleneimine) functionalized MWCNT results in a lower wear rate of 4.6×10^{-5}, compared to $10.6\times10^{-5} mm^3 Nm^{-1}$. However, the friction coefficient fell from 0.8 to 0.6, which is still very high.[25]

Epoxy nanocomposites have gained prominence in mechanical friction applications due to their tunable properties, yet achieving a balance between wear resistance and mechanical strength remains a critical challenge. The incorporation of nanofillers into epoxy matrices aims to enhance tribological performance, including reduced friction and wear and mechanical attributes, including tensile strength, and elastic modulus, but trade-offs often arise, as evidenced by extensive research.[26] Studies demonstrate that nanofillers like Al_2O_3, SiO_2, MWCNTs, and graphene derivatives improve wear properties, yet mechanical degradation occurs due to agglomeration or poor interfacial bonding. For instance, epoxy with 3 wt.% Al_2O_3[26] via ultrasonication achieves improved wear resistance, but a low tensile strength of 40.79 MPa, suggesting agglomeration disrupts load transfer. Similarly, 5 wt.% SiO_2[27] via solution mixing yields a high hardness and elastic modulus (3.5 GPa), but an increased wear rate indicates matrix compromise. Epoxy with 0.5 wt.% MWCNTs[28] shows enhanced wear resistance, yet its tensile strength (45 MPa) and elastic modulus (1.73 GPa) remain suboptimal, reflecting dispersion challenges.

Conversely, functionalized graphene offers better balance. Epoxy with 4.5 wt.% GNPs[29] improves wear, but limits tensile strength to ≈47.5 MPa, while 0.5 wt.% modified GO[30] achieves a low wear rate (3.0×10^{-5} mm^3 Nm^{-1}) with low tensile strength (≥35 MPa). These examples underscore the importance of optimizing filler type, concentration, and processing (e.g., ultrasonication, casting) to mitigate trade-offs. Balancing wear and mechanical properties are vital for durable, multifunctional composites, driving research toward hybrid nanofiller systems and advanced dispersion techniques. Understanding and optimizing these properties is critical because epoxy composites are often deployed in demanding environments such as automotive components, aerospace structures, and industrial machinery where they must withstand mechanical loads while resisting wear and friction-induced degradation.

Previous studies have extensively explored the wear reduction of MWCNT/epoxy composites, demonstrating that nanotube clustering prevents effective penetration into the material.[23] Additionally, research has highlighted the role of functionalization in reducing friction and wear.[24] However, these studies have not thoroughly explained the underlying mechanism of self-lubrication facilitated by MWCNTs. While Sakka et al.[31] proposed a hypothetical model describing the self-lubrication process of epoxy/MWCNT composites, suggesting that MWCNTs act as self-lubricating agents by breaking down under load and forming graphitic lubrication layers, this concept remains largely unverified with direct experimental evidence.

This study aims to systematically investigate the structural transformations and wear mechanisms of functionalized MWCNTs (P-MWCNTs, COOH-MWCNTs, NH_2-MWCNTs, and Silane-modified MWCNTs) under varying loads and sliding speeds. Unlike previous studies, this research uniquely integrates XRD and TEM to reveal critical structural changes, including nanotube flattening, fragmentation, rupturing, and friction-induced graphitization. The novelty of this work lies in establishing a direct link between MWCNT functionalization, dispersion quality, and the significant enhancement of mechanical and tribological properties. Through functionalization, covalent bonding and improved interfacial adhesion between MWCNTs and the epoxy matrix are achieved, optimizing stress transfer and reinforcing the matrix. This improved bonding contributes to enhanced hardness, tensile strength, ductility, and reduced brittleness, resulting in superior mechanical performance. The functionalization process also significantly influences wear mechanisms, including abrasive, fatigue, delamination, and adhesive wear resistance. For instance, the formation of protective tribofilms, particularly by COOH-MWCNTs, reduces wear rates and COF through friction-induced graphitization, which acts as a self-lubricating layer.

The integration of XRD and TEM analyses provides unprecedented insight into how functionalized MWCNTs undergo structural modifications under frictional conditions. These findings demonstrate that functionalization plays a pivotal role in optimizing wear mechanisms by enhancing load distribution, minimizing agglomeration, and promoting the formation of lubricating films. Furthermore, this study establishes a comprehensive framework to improve the tribological and mechanical performance of epoxy composites for high-performance applications such as automotive bushings, industrial sliding components, and protective coatings. The insights gained will facilitate the development of more durable and efficient self-lubricating composites tailored for advanced tribological systems.

2. Experimental Section

2.1. Materials

Bisphenol A/epichlorohydrin 50–70 wt.% epoxy resin, Isophoronediamine (3-aminomethly-3,5,5-trimethyl-cyclohexylamine) 50–60 wt.% curing agent, and the mold release agent were purchased from Norski, Plimmerton, New Zealand. Silane coupling agent KH-550 $(C_2H_5O)_3Si_3H_6NH_2$ and H_2SO_4 and HNO_3 – 63w% Concentration, Ethanol (CH_3CH_2OH) and acetone $(CH_3)_2CO$ with 99.9% purity were obtained from Merck Life Science Ltd., Auckland, New Zealand. Pristine MWCNTs and NH_2 functionalized MWCNTs had ≈10 µm in length and diameter less than 40 nm, and purity >98% was obtained Adnano Technologies Pvt.Ltd., Karnataka, India. **Table 1** list the material characteristics.

2.2. Functionalization of MWCNT

30 mg of P-MWCNTs were treated with a 3:1 mixture of concentrated sulfuric and nitric acids under continuous magnetic stirring at 40 °C for 10 h. The mixture was filtered, and the residue was repeatedly washed with deionized water[13]. **Table 2** provides more details. The purification process was further conducted by repeated washing, followed by high-speed centrifugation at 1000 rpm for 7 min until the pH of the decanted solution reached

Table 1. Characteristics and sources of materials used in epoxy composite fabrication.

Material	Description & Purity	Supplier	Use for
Epoxy Resin (Bisphenol A/epichlorohydrin)	50–70 wt.%, High purity	Norski, Plimmerton, New Zealand	Matrix material for composites
Curing Agent (Isophoronediamine) (3-aminomethyl-3,5,5-trimethyl-cyclohexylamine)	50–60 wt.%, High purity	Norski, Plimmerton, New Zealand	Crosslinking agent for epoxy resin
Mold Release Agent	High purity	Norski, Plimmerton, New Zealand	Prevents epoxy adhesion to molds
Silane Coupling Agent (KH-550)	$(C_2H_5O)_3Si_3H_6NH_2$, High purity	Merck Life Science Ltd., Auckland, New Zealand	Functionalization of MWCNTs
Sulfuric Acid (H_2SO_4)	63 wt.% Concentration		Acid treatment for MWCNT functionalization
Nitric Acid (HNO_3)	63 wt.% Concentration		Acid treatment for MWCNT functionalization
Ethanol (CH_3CH_2OH)	99.9% Purity		Solvent for MWCNT processing
Acetone ($(CH_3)_2CO$)	99.9% Purity		Cleaning and processing solvent
Pristine MWCNTs	Length: ≈10 µm, Diameter: <40 nm, Purity: >98%	Adnano Technologies Pvt. Ltd., Karnataka, India	Reinforcement in epoxy composites
NH_2 Functionalized MWCNTs	Length: ≈10 µm, Diameter: <40 nm, Purity: >98%	Adnano Technologies Pvt. Ltd., Karnataka, India	Improved dispersion & bonding in composites

neutrality (pH 7.0). After purification, the COOH-MWCNTs were dried in a vacuum oven at 90 °C for 15 h to ensure complete removal of moisture and residual solvents.

A silane-absolute ethanol solution was prepared at a concentration of 0.001 g mL^{-1}, with the KH-550 silane coupling agent amount set to 10% by weight of the COOH-MWCNTs. The dried 15 mg of COOH-MWCNTs were added to the solution and stirred with a magnetic stirrer at 60 °C for 30 min, followed by sonication for 1 hour to ensure dispersion.[32] During this process, covalent Si-O-C bonds were formed between the carboxyl groups on the MWCNTs and the silane agent. Residual solvents were removed by shaking the MWCNTs in acetone, followed by drying in a vacuum oven at 70 °C for 8 h. Finally, the sample underwent an additional drying step in a vacuum oven at 90 °C for 15 h to ensure complete removal of any remaining moisture and solvents **Figure 1** shows the material and process graphical representation.

2.3. Preparation of Composite

The epoxy composites were prepared using an open mold process, incorporating functionalized P-MWCNTs, COOH-MWCNTs, NH_2-MWCNTs, and Silane-modified MWCNTs as reinforcements. To ensure accurate mixing and homogeneity, the MWCNTs were precisely measured to achieve weight fractions of 0.1, 0.2, 0.3, 0.4, and 0.5 wt.%. **Table 3** lists the mixing quantities. The compositions were selected based on a comprehensive literature review, which indicated optimal tribological performance within the range of 0.1 to 0.5 wt.% MWCNTs.[12–15] Beyond 0.5 wt.%, the viscosity of the epoxy resin increased drastically, making handling and processing extremely difficult. The MWCNTs were initially dispersed into the epoxy resin by mechanical stirring for one hour, followed by ultrasonication for 20 min by Sonics Materials VC-505-220, Vibra Cell, high-intensity ultrasonicator (12 mm titanium tip of a 20 kHz ultrasonic horn

Table 2. Materials and process parameters used for functionalization.

Step	Parameters	Purpose
Acid Treatment (COOH-MWCNTs)	**P-MWCNTs**: 30 mg	Introduce COOH groups on MWCNTs.
	Acid Mixture: 3:1 Sulfuric Acid (H_2SO_4): 37.5 ml Nitric Acid (HNO_3):12.5 ml Deionized Water: 200ml	
	Stirring: Magnetic stirring at 40 °C for 10 h	
	Purification: Repeated washing with deionized water	Remove residual acids.
	Centrifugation: 1000 rpm for 7 min (until pH = 7)	Remove residual acids. Achieve neutral pH (pH 7.0).
Drying (COOH-MWCNTs)	**Vacuum Oven**: 90 °C for 15 h	Remove moisture and residual solvents.
Silane Functionalization (Silane-modified MWCNTs)	**COOH-MWCNTs**: 15 mg	For covalent Si-O-C bonds
	KH-550 Silane Agent: 1.5 mg	
	Solvent: Ethanol 150 ml	
	Stirring: Magnetic stirring at 60 °C for 30 min	Initial mixing.
	bath Sonication: 1 hour	Ensure reaction.
Washing & Drying (Silane-modified MWCNTs)	**Washing**: Shaking with acetone	Remove residual solvents.
	Drying: Vacuum oven at 70 °C for 8 h, then 90 °C for 15 h	Complete removal of moisture and solvents.

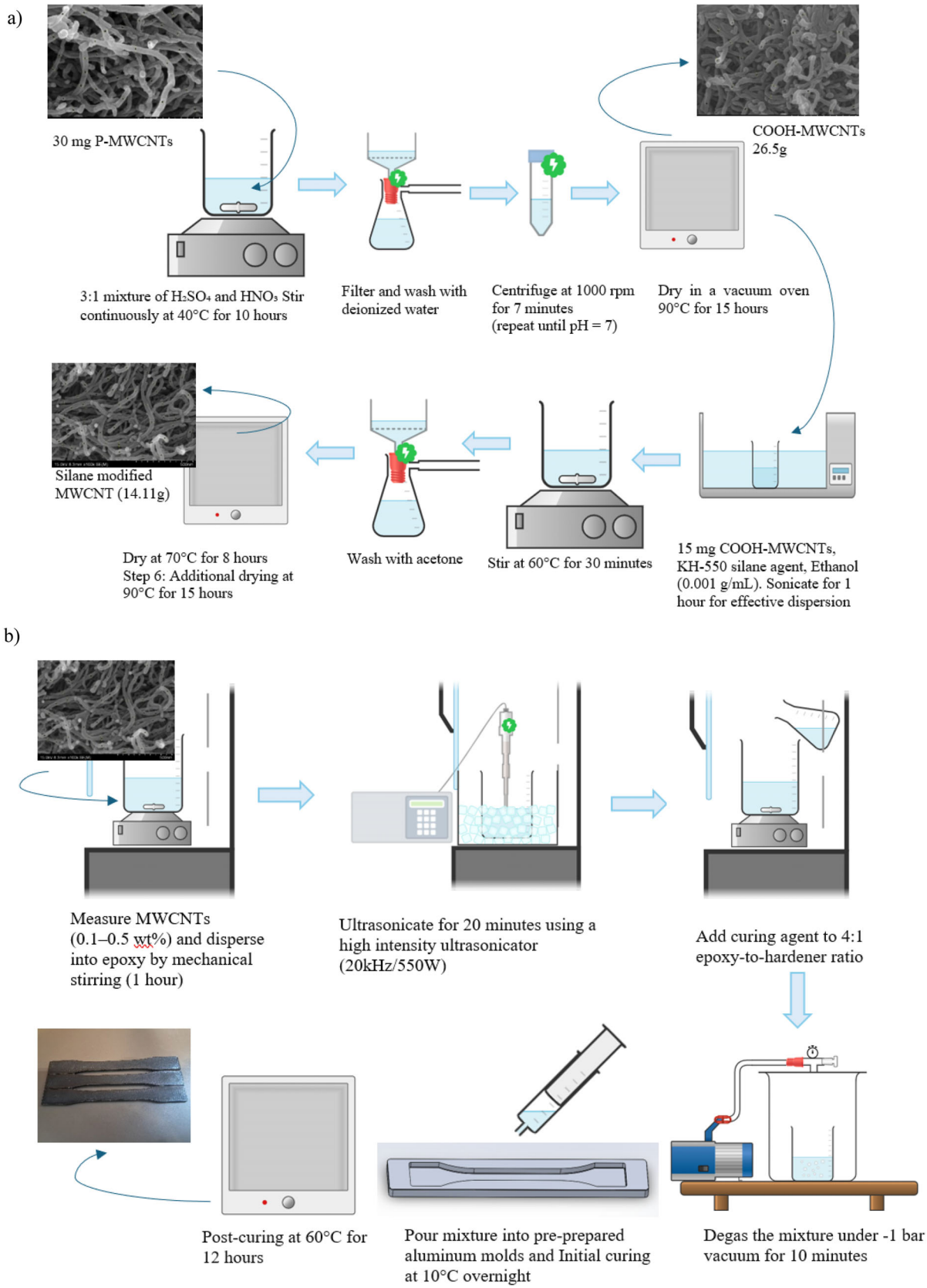

Figure 1. a) Functionalization process of MWCNTs to obtain COOH-MWCNTs and silane-modified MWCNTs and b) Composite preparation process.

Table 3. Resin mixing chart for each composite MWCNT and each F-MWCNTs.

MWCNT Weight Fraction (wt%)	Epoxy Resin (g)	Curing Agent (g)	MWCNTs (g)
0.1	99.9	24.98	0.1
0.2	99.8	24.95	0.2
0.3	99.7	24.93	0.3
0.4	99.6	24.90	0.4
0.5	99.5	24.88	0.5

transducer with nominal power of 550 W with a nominal output frequency of 20 kHz). This dual-stage process facilitated uniform dispersion of the MWCNTs in the epoxy matrix.

After dispersion, the curing agent, isophoronediamine, was added to achieve a 4:1 epoxy-to-hardener ratio. The mixture underwent degassing under a vacuum of −1 bar for 10 min to eliminate entrapped air. The degassed mixtures were then poured into pre-prepared aluminum molds, which had been smoothed with a scotch pad and treated with a mold release agent to ensure a uniform surface finish. The composite mixing process control parameters are listed in **Table 4**. The curing process followed a two-step cycle: initial curing at 10 °C overnight, followed by post-curing at 60 °C for an additional 12 h. This curing protocol, based on the epoxy supplier's data sheet, ensured optimal crosslinking and mechanical integrity. The curing process is detailed in **Table 5**. The cyclic curing process minimized the risks of temperature overshoot and non-uniform curing, thereby preventing resin degradation, void formation, and incomplete crosslinking. Control samples without MWCNTs were fabricated for baseline comparisons to evaluate the mechanical and tribological influence of functionalized MWCNTs on the composites.

2.4. Test Procedure

Tensile specimens were fabricated in accordance with EN ISO 527-2 type 1b geometry.[33] The dog-bone-shaped specimens had dimensions of 4 mm in width, 150 mm in length, and a 50 mm gauge length. Tensile testing was carried out using a computer-controlled servo-hydraulic universal testing machine with a maximum load capacity of 50 kN, operating at a testing rate of 1.5 mm min^{-1}. Stress-strain curves were recorded to determine ultimate tensile strength, Young's modulus, and elongation of the epoxy composites, following ISO 527-1 standards.[34] Hardness testing was performed using a type D durometer in accordance with ASTM D2240,[35] and average values were obtained from five replicates for each condition.

Table 5. Curing process.

Stage	Temperature	Duration	Purpose
Initial curing	10 °C	Overnight	Ensure gradual curing to prevent temperature overshoot.
Post curing	60 °C	12 hrs	Enhance crosslinking and mechanical integrity.

The functionality of the MWCNTs was verified using Fourier Transform Infrared Spectroscopy (FTIR) and TEM/EDX to confirm the presence of functional groups and elements such as carboxyl, amine, and silane modifications. This ensured proper functionalization and further the ability of uniform dispersion within the epoxy matrix. Tribological specimens, designed for wear testing, were rectangular plates with dimensions of 5 mm in height, 40 mm in length, and 25 mm in width. Wear tests were conducted using a Rtec tribometer MFT-5000 (Rtec Instruments, USA) under dry sliding conditions. The counter surface was a chromium steel ball with a diameter of 10 mm and a surface roughness of 2.5 µm. Tests were performed at a controlled temperature of 24 °C and 60% relative humidity. Composite surfaces and counter-balls were cleaned with acetone before testing to eliminate contaminants.

Test parameters were selected to replicate conditions exceeding those typical for industrial polymer bearings.[36,37] Sliding frequencies of 2, 5, and 8 Hz were applied, resulting in sliding speeds of 0.02, 0.07, and 0.2 m s^{-1}. Normal loads of 5N, 10N, and 1N created maximum applied pressures of 121.73, 153.39, and 175.58 MPa, respectively, as calculated using Hertzian contact theory.[38] Test durations of 68, 95, and 248 min were chosen to achieve a constant sliding distance of 400 m. Each condition was repeated three times to ensure reproducibility, and the average coefficient of friction (COF) was calculated with associated standard errors. Post-test analyses included scanning electron microscopy (SEM) (Hitachi SU-70) with samples sputter-coated with platinum for 60 s using a Hitachi E-1045 ion sputter. SEM images were obtained at an accelerating voltage of 10 kV.

Prior to testing, all specimens were polished with 1200-grit sandpaper to standardize surface conditions. Wear volume was determined by measuring track width and depth using a surface profilometer (Taylor Hobson Form Talysurf 50) with a 4 µm diamond stylus. XRD analysis of the wear debris was conducted to evaluate defect evolution and crystal structure changes of MWCNTs during wear. XRD patterns were obtained using a PANalytical Empyrean powder diffractometer at 45 kV and 40 mA. A standard Cu X-ray source with a $K\alpha_1$ wavelength of 1.5418 Å was used. Scans were conducted over a 2θ range of 5-−80° with a step size

Table 4. Composite mixing parameters.

Stage	Temperature	Duration	Purpose
Dispersion Process	Mechanical Stirring: 500 rpm	1 hour	initial dispersion of MWCNTs.
	Ultrasonication: (20 kHz, 550 W)	20 min	Ensure homogeneous dispersion.
Degassing Process	Vacuum: -1 Bar	10 min Until the cessation of bubble formation	Remove all the entrapped air to avoid void formation

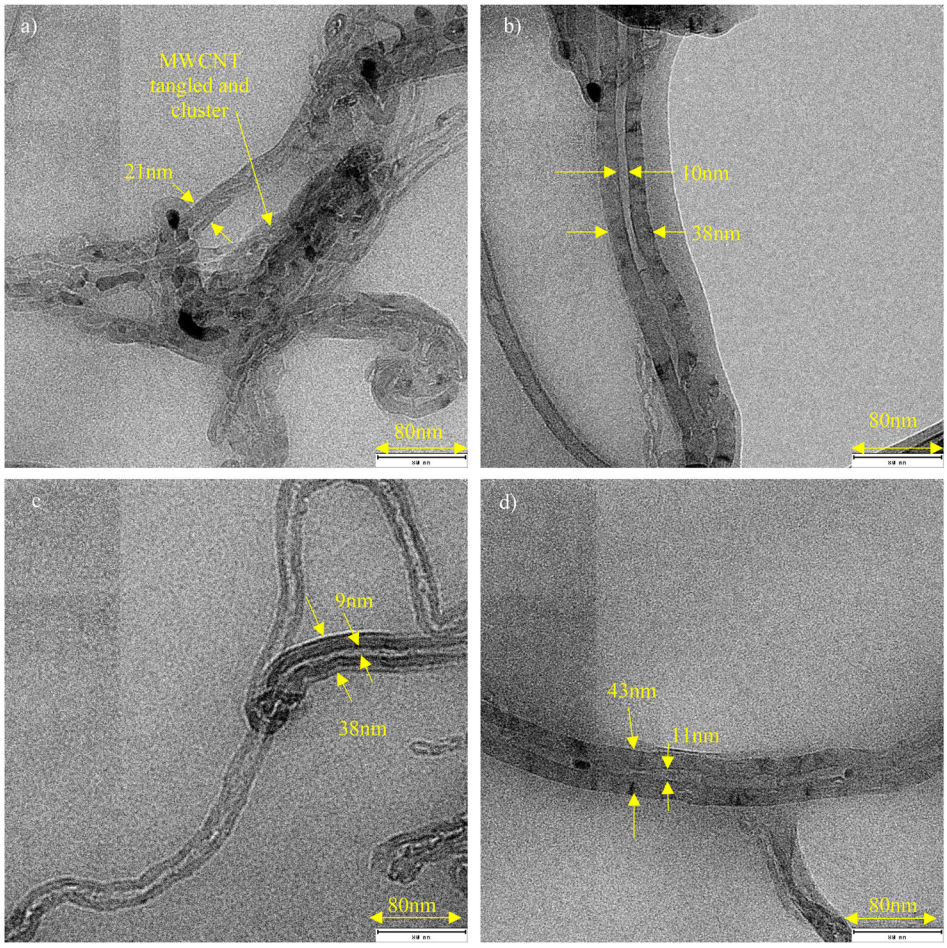

Figure 2. TEM image of dry powder a) P-MWCNTs and their functionalized derivatives; b) COOH-MWCNT; c) NH_2-MWCNT; and d) Silane-modified MWCNT.

of 0.013°. TEM was conducted to examine the fragmentation and graphitization of MWCNTs during the wear process. This analysis provided insights into structural integrity, changes in morphology, and the extent of breakage or shortening of MWCNTs under applied stresses. TEM imaging was performed at high resolution, allowing detailed observation of the wear-induced alterations in MWCNT structure, within the wear debris.

3. Results and Discussion

3.1. TEM Observations

Figure 2 presents the TEM micrographs of P-MWCNTs and their functionalized derivatives COOH-MWCNTs, NH_2-MWCNTs, and silane-modified MWCNTs. A distinct morphological difference is observed between the pristine and functionalized MWCNTs, particularly in the increased wall thickness of the functionalized nanotubes.

The P-MWCNTs exhibit an outer diameter of ≈20–25 nm, with an inner diameter ranging between 9 and 10 nm, maintaining a tangled and hollow tubular structure. In contrast, the functionalized MWCNTs demonstrate a notable increase in wall thickness, with an outer diameter extending to ≈38–40 nm. This increase can be attributed to the surface modifications induced by functionalization processes, which introduce additional chemical moieties on the nanotube walls. Such modifications likely enhance interfacial interactions with the surrounding epoxy matrix and better dispersion, thereby influencing the composite's tribological and mechanical performance.

These observations provide critical insights into how functionalization alters the physicochemical structure of MWCNTs, which may have significant implications for their dispersion behavior, load-bearing capacity, and self-lubrication mechanisms in epoxy-based composite systems.[39]

3.2. FTIR Characterization of MWCNT Functionalization

Figure 3 FTIR spectra, revealing a comprehensive comparison of P-MWCNTs and their functionalized derivatives, COOH-MWCNTs, NH_2-MWCNTs, and silane-modified MWCNTs. Each spectrum delineates distinct peaks that correspond to the vibrational modes of functional groups introduced during the functionalization operations, as well as the intrinsic characteristics of P-MWCNTs. Figure 3a the aromatic C=C stretching vibration, a signature of sp^2-hybridized carbon in the hexagonal lattice of

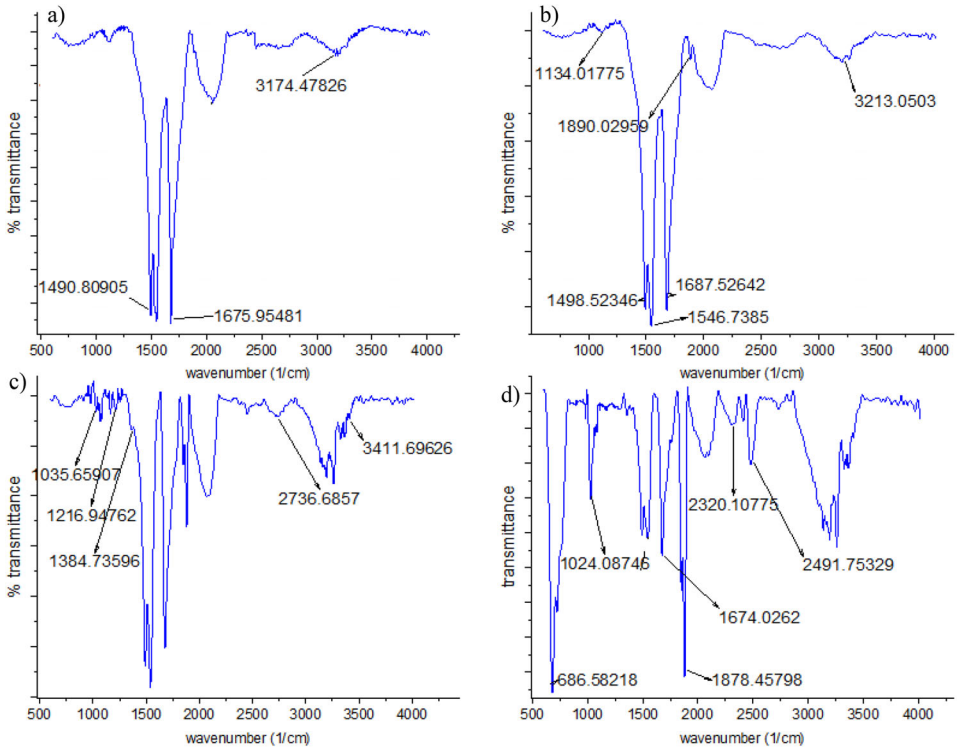

Figure 3. FTIR spectra analysis (500 cm^{-1} to 4000 cm^{-1}) of dry powder a) P-MWCNTs and their functionalized derivatives; b) COOH-MWCNT; c) NH_2-MWCNT; and d) Silane-modified MWCNT.

MWCNTs, is represented by a peak at 1490 cm^{-1}. Minor lattice defects or adsorbed atmospheric species are suggested by an attenuated peak at 1675 cm^{-1}. The broad peak at 3174 indicates the presence of O-H stretching, which may be the result of atmospheric condensation adsorbed onto the surface.[40,41]

Figure 3b COOH-MWCNTs are characterized by a prominent peak at 1687 cm^{-1}, which corresponds to the C═O stretching vibration of the carboxyl group. The presence of hydroxyl groups from the functionalization process is confirmed by the broad peaks at 3213 and 1890 cm^{-1}, which are indicative of O-H stretching vibrations. Vibrations associated with oxygen-containing hydroxyl (-OH) ambient moisture are represented by additional peaks at 1134 cm^{-1}.[42–44] The FTIR spectrum of NH_2-MWCNTs in Figure 3c displays unique peaks that validate successful amine functionalization. A prominent peak at 3411 cm^{-1}, associated with N-H stretching vibrations, serves as a crucial diagnostic of main or secondary amine groups on the MWCNT surface. The signal at 2736 cm^{-1} corresponds to C-H stretching vibrations of alkyl groups, likely introduced during functionalization or as leftover reagents. Moreover, the peaks at 1384 and 1216 cm^{-1} correspond to C—N stretching vibrations linked to amine and amide groups, respectively, so offering additional confirmation of functionalization. The peak at 1035 cm^{-1}, indicative of C—N stretching, confirms the effective integration of amine groups. The spectrum characteristics underscore the structural alterations attained via amine functionalization, rendering NH_2-MWCNTs appropriate for improved interactions with polymers and other functional materials.[45–47]

Figure 3d Silane-modified MWCNTs demonstrates successful chemical modification through the introduction of various functional groups from the silane coupling agent (KH-550). The characteristic peaks at 686.58 cm^{-1} (Si–O–Si stretching) and 1024.09 cm^{-1} (Si–O–C stretching) confirm the formation of covalent bonds between the silane agent and the MWCNT surface, indicating effective functionalization. A weak band ≈1500 cm^{-1} corresponds to C═C stretching, confirming that the intrinsic graphitic structure of MWCNTs is preserved even after functionalization. Peaks at 1674.03 and 1878.46 cm^{-1} are attributed to C═O stretching vibrations, which may arise from partial oxidation or interactions with the coupling agent. The presence of a broad peak at 2320.11 cm^{-1} is linked to $–NH_2$ stretching vibrations, demonstrating successful incorporation of amine groups from the silane coupling agent.[48,49] Additionally, the spectrum shows a weak band at ≈2750 cm^{-1} (C–H stretching), suggesting minor organic residues or incomplete reactions, while the broad peaks at 3250 cm^{-1} (N–H stretching) and 3500 cm^{-1} (O–H stretching) are indicative of amine functional groups and potential moisture absorption, respectively.[50] A peak at 2491.75 cm^{-1} associated with Si–H stretching implies incomplete hydrolysis of the silane agent during functionalization.[22]

3.3. MWCNTs Dispersion and Mechanical Properties of Composites

The comprehensive explanation of the impact of MWCNT functionalization on epoxy composites is achieved through the integration of fracture surface SEM analysis and mechanical strength

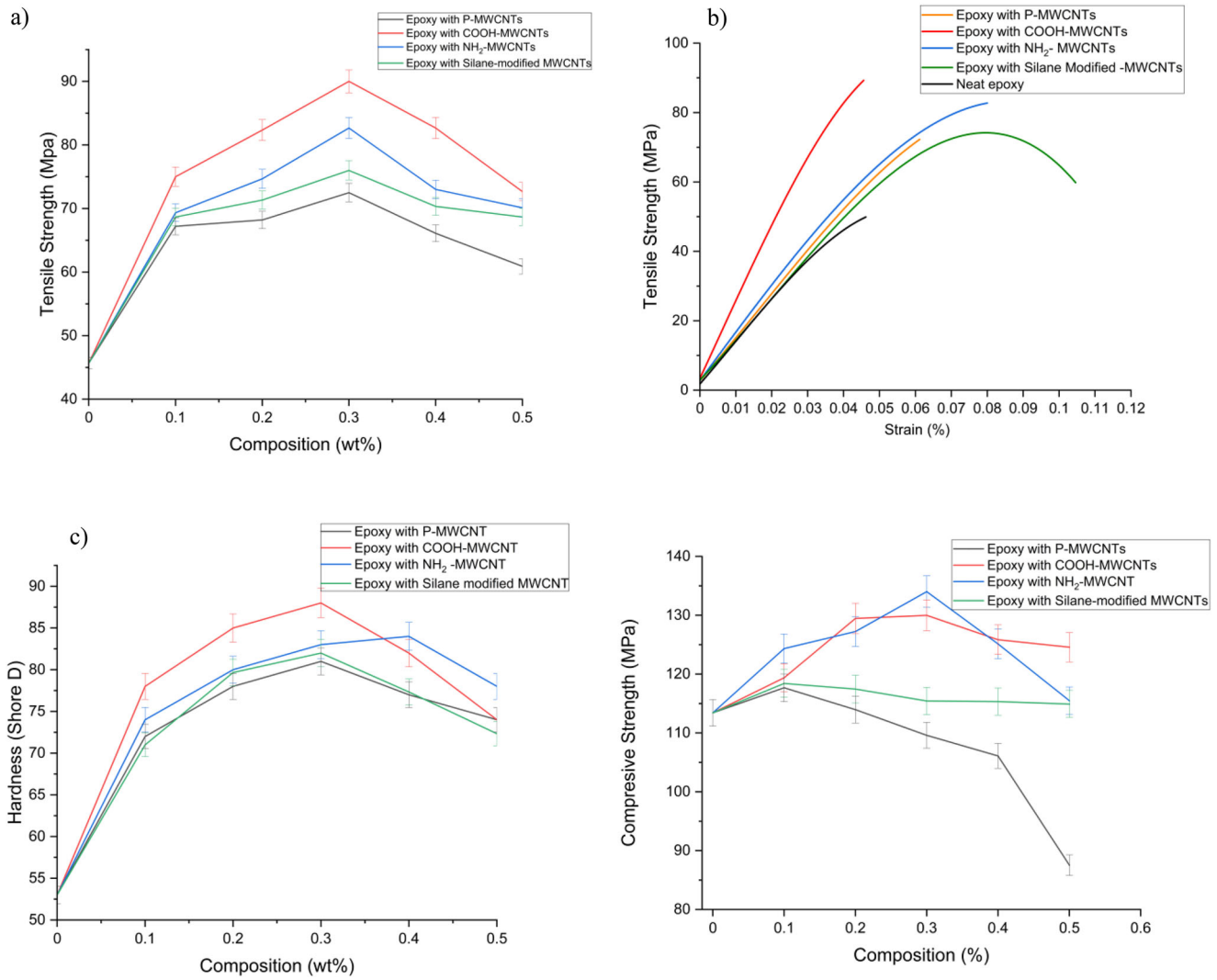

Figure 4. a) Tensile strength distribution P-MWCNT, COOH-MWCNT, NH_2 -MWCNT and Silane-modified MWCNT epoxy composite with their composition; b) Tensile strength versus Strain curve for P-MWCNT and their derivative MWCNTs composites at 0.3wt% and c) Hardness; d) Compressive strength.

data. The mechanical properties that are observed are directly correlated with these structural enhancements, as illustrated in **Figure** 4a–c, with the fiber distribution of pristine and functionalized MWCNTs illustrated in SEM images (**Figure 5**), which emphasize the critical role of functionalization in improving interfacial bonding and dispersion.

The tensile strength of epoxy composites increases as the MWCNT content increases, reaching a maximum of 0.3 wt.% for all functionalized MWCNTs varieties (Figure 4a). Agglomeration reduces the effective load transfer beyond this composition, resulting in a decrease in strength. The COOH-MWCNT composites exhibit the highest tensile strength, underscoring the efficacy of carboxyl groups in enhancing interfacial adhesion. The tensile strength versus strain curves (Figure 4b) show the increased ductility of silane-modified MWCNTs, which exhibit a superior strain capacity compared to other functionalized variants. COOH-MWCNTs maintain the highest tensile strength, while NH_2-MWCNTs exhibit a balanced performance in terms of ductility and strength. The reinforcing benefits of MWCNT incorporation are underscored by the clean epoxy curve, which reflects the lowest strength and strain.[51,52]The hardness (Figure 4c) of the material increases as MWCNT is added, reaching a maximum at 0.3 wt.%. The maximum hardness is exhibited by COOH-MWCNTs (88 ShoreD) due to their exceptional interfacial bonding and dispersion. Silane-modified and NH_2-functionalized MWCNTs also improve hardness in comparison to pristine composites. However, agglomeration and diminished performance result from excessive filler content (>0.3 wt.%). Figure 4d shows the compressive strength of epoxy composites reinforced with various MWCNTs (P-MWCNTs, COOH-MWCNTs, NH_2-MWCNTs, and Silane-modified MWCNTs) across compositions from 0 to 0.5%. The COOH-MWCNT composite exhibits the highest compressive strength (130 MPa) at 0.3%, followed by NH_2-MWCNTs with a peak (134 MPa) at the same composition. P-MWCNTs show a continuous decline beyond 0.1%, indicating poor dispersion. Silane-modified MWCNTs maintain

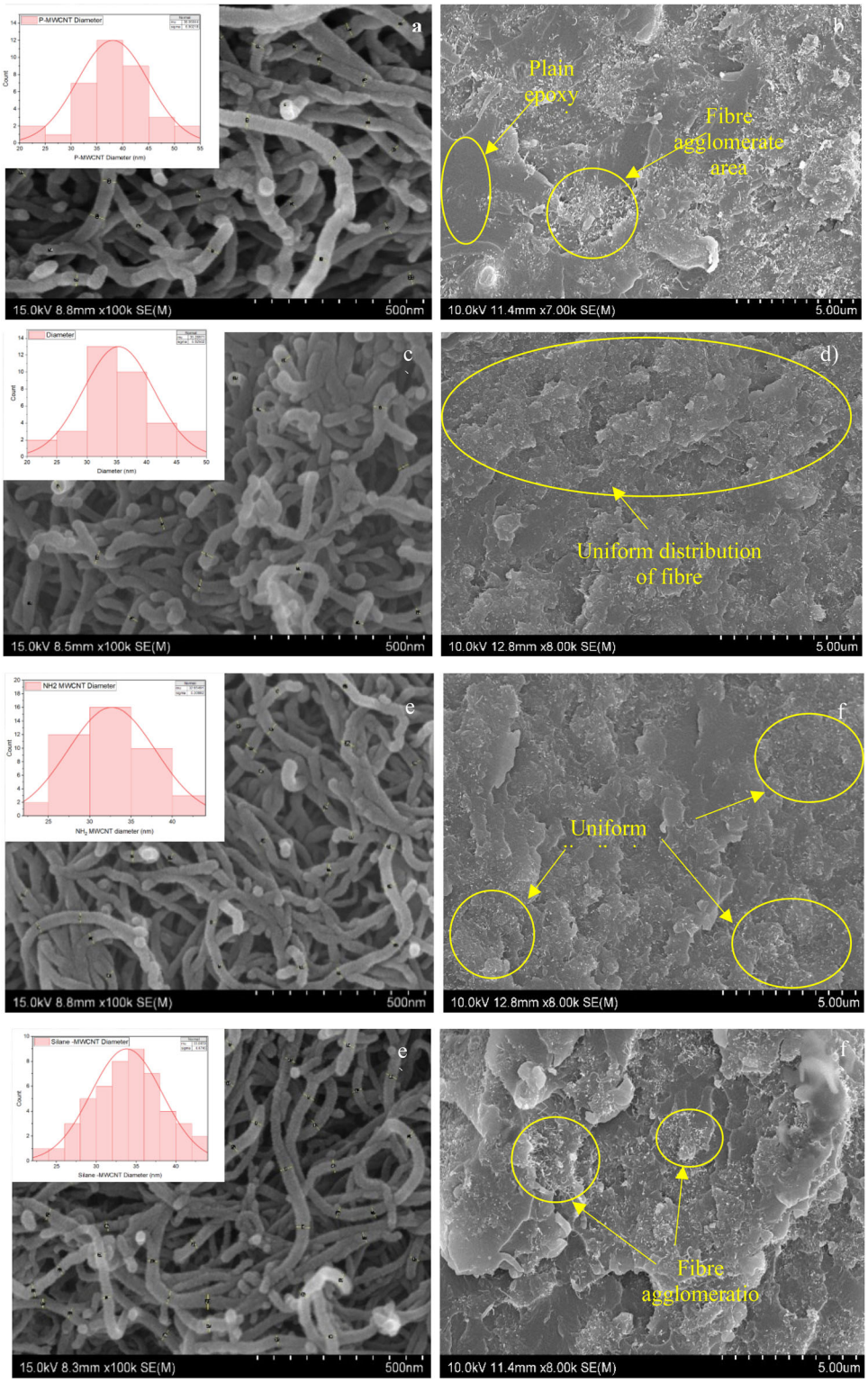

Figure 5. SEM images and fiber width distribution of pristine and functionalized (MWCNTs) within an epoxy matrix: a,b) P-MWCNTs; c,d) COOH-MWCNTs; e,f) NH_2-MWCNTs; and g,h) silane-modified MWCNTs.

Table 6. Tensile properties of neat epoxy and 0.3 wt.% MWCNT-reinforced epoxy composites.

Property	Neat epoxy	Epoxy with P-MWCNTs	Epoxy with COOH-MWCNTs	Epoxy with NH_2-MWCNTs	Epoxy with Silane-modified MWCNTs
Compressive Strength (Mpa)	45.68	72.50	90.00	82.67	76.00
Strain (%)	0.05	0.05	0.05	0.10	0.06
Elongation at break (%)	4.62	4.62	4.54	10.46	6.12
Young's Modulus (Mpa)	988.74	1569.26	1983.69	790.31	1241.83

stable performance but slightly decrease above 0.3%. The results suggest optimal performance at 0.3 wt.%, particularly for COOH-MWCNTs. **Table 6** presents the tensile properties of neat epoxy and epoxy composites reinforced with 0.3 wt.% of various functionalized MWCNTs. The data indicates that incorporating functionalized MWCNTs enhances the mechanical properties of epoxy composites, with COOH-MWCNTs showing the most significant improvement in tensile strength and Young's modulus (approximately by 50%). These findings highlight the impact of different MWCNT functionalizations on the mechanical properties of epoxy composites, influencing their potential applications based on required flexibility and stiffness.

P-MWCNTs in the SEM images (Figure 5a) demonstrate unfunctionalized fibers. Agglomeration and inconsistent dispersion in the epoxy matrix result from inadequate interfacial bonding, which is caused by the absence of functional groups (Figure 5b). As a result, the tensile strength and hardness of P-MWCNT composites are the lowest among the tested samples. The reinforcing potential is restricted by the poor load transmission that results from the weak van der Waals forces between the pristine fibers and the epoxy matrix.

COOH-MWCNTs show that carboxyl (COOH -MWCNTs) groups have been added through acid functionalization (Figure 5c). These functional groups make sure that the particles are spread out evenly in the matrix by improving the bonds between surfaces through covalent and hydrogen bonds. Given their maximum tensile strength (≈90 MPa at 0.3 wt.%), and hardness (≈88 Shore D), COOH-MWCNT composites are clearly well dispersed. The enhanced matrix interaction greatly increases the structural performance of the composite, therefore enabling efficient load transfer.[53,54] The amine functionalization (Figure 5e) fibers generate strong covalent connections with the epoxy during curing,[55] as evidenced by the consistent dispersion shown in Figure 5f. These results consistence with the tensile strength and hardness values, alien to NH_2-MWCNT composites. The tensile strength-strain relationship (Figure 4b) demonstrates that NH_2-MWCNT composites may preserve structural integrity under load, exhibiting a balance between ductility and reinforcement efficiency.

SEM images (Figure 5g,h) indicate silane-modified MWCNTs. Silane coupling agents establish Si-O-Si and Si-O-C covalent connections, enhancing compatibility with the epoxy matrix. Despite ongoing clustering resulting from limited grafting density or dispersion difficulties, silane-modified composites demonstrate enhanced strain capacity (Figure 4b) along with competitive tensile strength and hardness. This suggests that, despite localized clustering, the silane groups remarkably improve interfacial adhesion and load transfer. Enhancing the dispersion and bonding of MWCNTs within the epoxy matrix is a critical function of functionalization chemistry. The introduction of carboxyl groups (-COOH) by acid treatment facilitates hydrogen bonding and covalent interactions, which lead to improved load transfer. Mechanical reinforcement is further enhanced by the formation of covalent bonds during curing by NH_2 groups that are produced through amine functionalization. Silane coupling agents generate Si-O-Si and Si-O-C linkages, which improve compatibility and interfacial adhesion; however, dispersion challenges may persist. Functional groups minimize agglomeration and facilitate uniform distribution by decreasing fiber diameter and enhancing wettability. As demonstrated in composites functionalized with COOH and NH_2, this enhanced dispersion results in superior tensile strength, strain capacity, and hardness. Nevertheless, the mechanical performance is reduced by agglomeration, which occurs when the filler content exceeds 0.3 wt.%.

3.4. Friction and Wear Properties

The addition of 0.3 wt.% functionalized MWCNTs improves the tribological performance of epoxy composites under a wide range of sliding frequencies and normal loads, as shown in **Figure 6**.

Figure 6a shows that as the sliding frequency increases from 2 to 8 Hz, the specific wear rate of plain epoxy rapidly increases, reaching 0.40×10^{-6} mm^3 $N^{-1}{\cdot}m^{-1}$. Epoxy with COOH-functionalized MWCNTs had the lowest specific wear rate (SWR) of 0.07×10^{-6} mm^3 $N^{-1}{\cdot}m^{-1}$, resulting in an 82% drop. P-MWCNT, COOH-MWCNT, and NH_2-MWCNT reinforced epoxy composites all show similar patterns of increasing SWR with increasing sliding frequency. The NH_2-MWCNT ($0.08{\times}10^{-6}$ mm^3 $N^{-1}{\cdot}m^{-1}$) and Silane-modified MWCNTs ($0.09{\times}10^{-6}$ mm^3 $N^{-1}{\cdot}m^{-1}$) have lower SWR than the P-MWCNT ($0.15{\times}10^{-6}$ mm^3 $N^{-1}{\cdot}m^{-1}$). Functionalized MWCNT composites improve wear resistance by increasing dispersion, interfacial adhesion, and effective load transfer during sliding wear.

In Figure 6b, neat epoxy has the highest wear rate ($0.50{\times}10^{-6}$ mm^3 $N^{-1}{\cdot}m^{-1}$) at 15N, whereas COOH-MWCNTs have the lowest ($0.09{\times}10^{-6}$ mm^3 $N^{-1}{\cdot}m^{-1}$) at 10N resulting in an 82% reduction compared to neat epoxy. Silane-modified MWCNTs show slightly higher performance ($0.14{\times}10^{-6}$ mm^3 $N^{-1}{\cdot}m^{-1}$), while amine-functionalized MWCNTs and unmodified MWCNTs have intermediate values. Wear reduction is attributed to functionalized MWCNTs' ability to create a strong tribo-film, which reduces material loss.

In Figure 6c, neat epoxy has a high COF of 0.63 at 5N, which drops slightly at 10N due to higher asperity deformation but

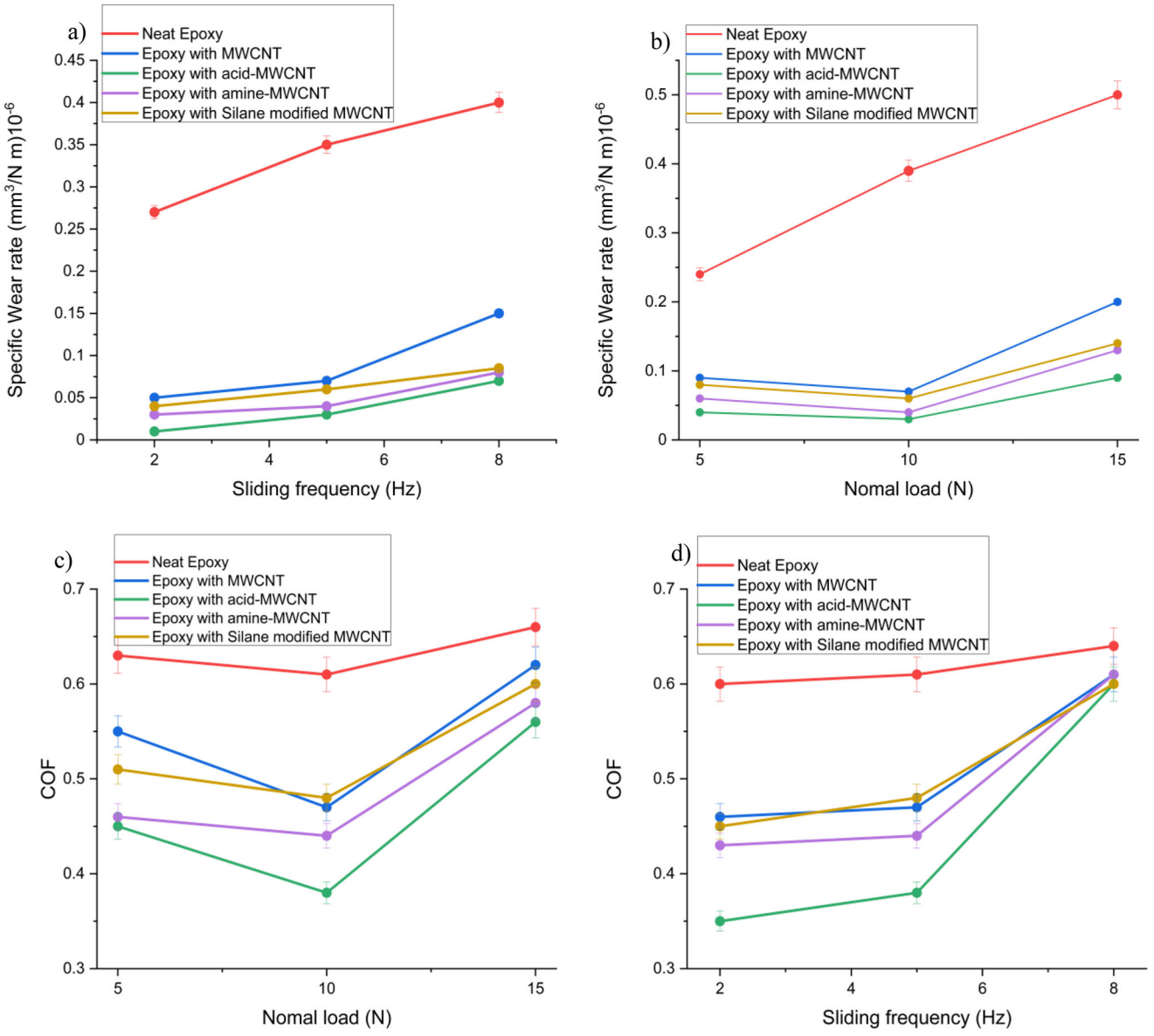

Figure 6. Effect of 0.3wt% of Functionalized MWCNTs loading on the tribological performance of epoxy composites: a) Specific wear rate versus sliding frequency under constant 10N normal load; b) Specific wear rate versus normal applied load at a constant sliding frequency of 5 Hz; c) COF versus normal applied load at a constant sliding frequency of 5 Hz. d) COF versus sliding frequency under a constant normal load of 10N.

climbs back to 0.66 at 15N. The COF for COOH-MWCNTs remained the lowest across all loads, measuring 0.37 at 10N (32% less than neat epoxy). All the functionalized types have comparable COF performance close to 0.60 at 15N, followed by P-MWCNTs and neat epoxy. The decrease in COF demonstrates the lubricating effect of functionalized MWCNTs, specifically COOH-MWCNTs.

Figure 6d, COF increases with sliding frequency in all samples due to improved adhesive contacts and frictional heat. Neat epoxy has the maximum COF of 0.61 at 5 Hz, while COOH-MWCNT composites have the lowest COF of 0.38 (37% reduction). NH_2-MWCNTs also provide excellent lubrication, with a COF of 0.44, followed by Silane- modified MWCNTs (0.47) and P-MWCNTs (0.47).

COOH-MWCNTs consistently outperform neat epoxy in terms of tribological performance, reducing SWR by up to 73% and COF by 35%, respectively. Silane-modified MWCNTs perform similarly, emphasizing the importance of functionalization in improving epoxy composites' wear resistance and self-lubrication capabilities. Neat epoxy has the weakest performance due to its brittle nature and lack of lubricating mechanisms.

3.5. Wear Mechanisms

Figure 7 shows SEM images of the wear mechanisms and tribological behavior of epoxy composites with different MWCNT functionalizations.

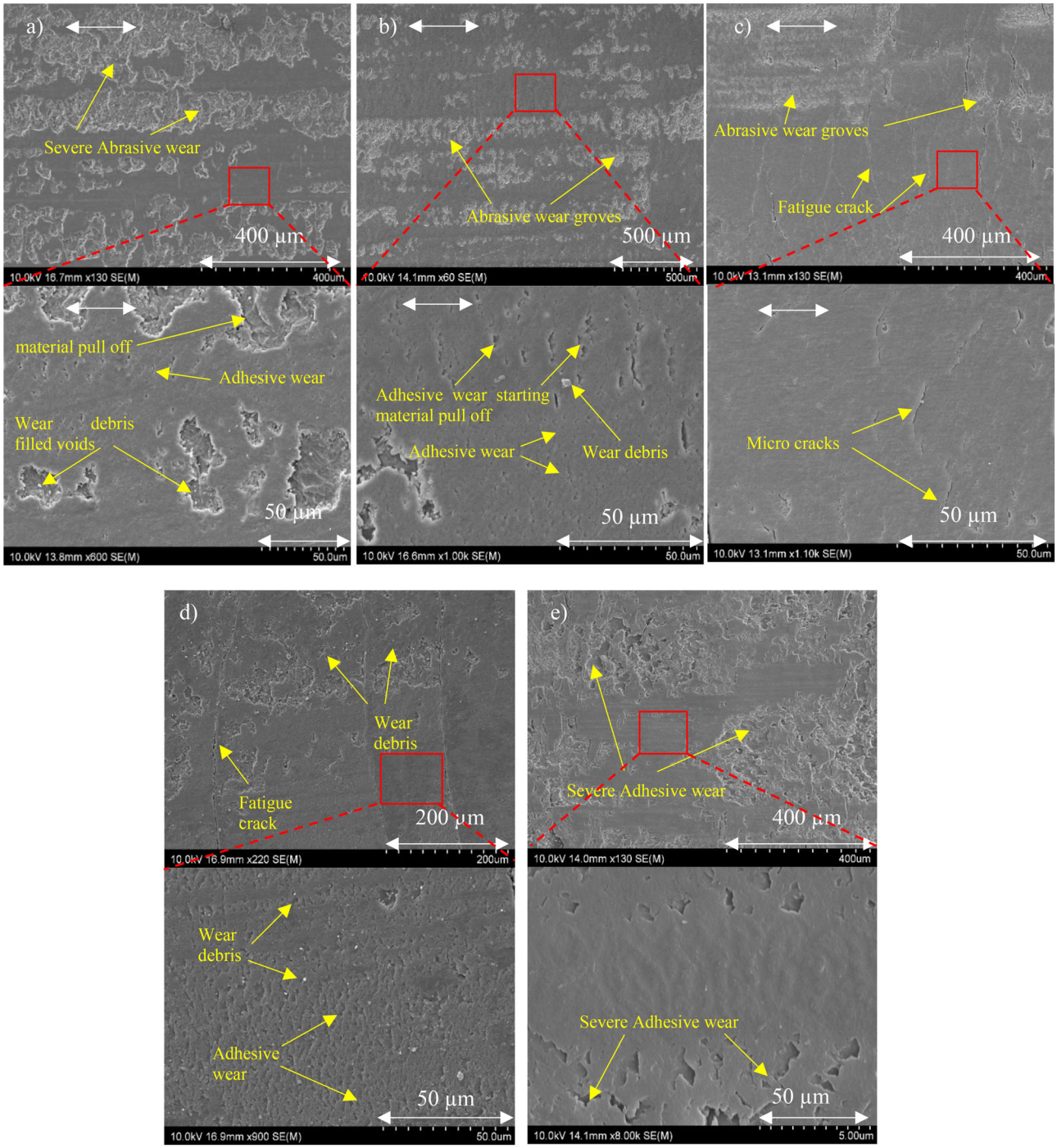

Figure 7. SEM images of wear tracks of samples tested under 10N/5 Hz sliding condition after 400m with different magnifications a) Neat epoxy; b) Epoxy with P-MWCNT; c) Epoxy with COOH-MWCNT; d) Epoxy with NH_2-MWCNT and e) Epoxy with Silane modified Composites.

In Figure 7a for neat epoxy, the wear track exhibits severe abrasive wear, including noticeable grooves and material pull-off, indicating poor mechanical characteristics and excessive brittleness. The lack of reinforcements causes poor load distribution, resulting in deep wear grooves and voids filled with wear debris. The weak matrix fails under stress, leaving massive wear scars. In Figure 7b, epoxy with P-MWCNT shows that the addition of P-MWCNTs reduces the severity of wear grooves when compared to neat epoxy, indicating a moderate improvement in mechanical qualities. However, the lack of functional groups results in weak interfacial bonding, which limits stress transfer and causes considerable adhesive wear and debris formation.

Figure 7c shows epoxy with COOH-MWCNT. The wear track shows shallow abrasive wear grooves and fatigue cracks, indicating that the matrix is still brittle. The carboxylic (-COOH) functional groups strengthen the interfacial adhesion between

MWCNTs and the epoxy matrix, improving load transfer and tribofilm stability. Improved dispersion and stress distribution reduce material pull-off, emphasizing good tribological and mechanical properties.

In Figure 7d, epoxy with NH_2-MWCNT improves the ductility of the matrix, and at the same time, it can be seen that the adhesive wear is dominant in the higher magnification. In Figure 7e, epoxy with Silane-modified MWCNT exhibits a high susceptibility to adhesive wear, resulting in higher strain under stress and fewer wear scars and debris. The silane coupling agent forms covalent bonds with both the MWCNT surface and the epoxy matrix, creating a stable interfacial bond. However, the extreme matrix ductility, as shown in Figure 4b, is again leading to severe adhesive wear that makes it very different from COOH-MWCNT and NH_2-MWCNT tribological performance.

In conclusion, the functionalization of MWCNTs significantly enhances wear resistance by improving dispersion, interfacial bonding, and tribofilm formation. Among the studied composites, COOH-MWCNT and NH_2-MWCNT demonstrate superior performance due to their combined mechanical reinforcement and lubricating effects. In contrast, neat epoxy exhibits poor wear resistance due to its inherent brittleness, which promotes excessive abrasive wear. Meanwhile, silane-modified MWCNTs result in excessive matrix ductility, leading to dominant adhesive wear mechanisms.

Figure 8 presents the EDS elemental analysis of the wear track surfaces of various epoxy composites tested under 10N/5 Hz sliding conditions over a total sliding distance of 400m. The analysis shows the elemental composition of carbon (C), oxygen (O), nitrogen (N), silicon (Si), and sulfur (S) on the worn surfaces. For the neat epoxy surface, Figure 8a, the composition mainly includes C and O, with a moderate oxygen percentage (4%), indicating the epoxy with minimal contamination. The MWCNT/epoxy composite in Figure 8c shows slightly higher oxygen content (6.01% to 7.28%), suggesting partial oxidation during sliding. The COOH-MWCNT/epoxy composite in Figure 8d displays improved high oxygen content (7.16% to 8.12%), and the presence of Si in minimal, indicating limited contamination during the wear sliding by counterpart. The NH_2-MWCNT/epoxy composite (Figure 8e) shows oxygen content ranging from 6.12% to 7.02%, which is relatively lower but indicates adhesive. The Silane-modified MWCNT/epoxy composite in Figure 8f shows the presence of Si, S, and K along with C and O, with oxygen levels between 7.12% and 7.16%. The Si peaks likely result from the silane functionalization, contributing to enhanced interfacial bonding and wear resistance. The overall EDS analysis indicates that functionalized MWCNT composites generally demonstrate better oxidation resistance and improved wear performance compared to the neat epoxy matrix. However, the oxygen content remains a key factor to monitor for long-term tribological performance.

3.6. XRD Patterns

As can be observed in **Figure 9**, the X-ray diffraction (XRD) pattern of P-MWCNTs typically exhibits characteristic peaks indicative of their graphitic structure. A prominent peak $\approx 2\theta = 26°$ corresponds to the (002) reflection, representing the interlayer spacing of the graphitic planes. Another notable feature is the peak near $2\theta = 43°$, associated with the (100) reflection of the graphitic lattice. The splitting observed $\approx 2\theta = 42°$ in the XRD pattern can be attributed to the presence of both (100) and (101) reflections, which are closely spaced and may overlap, leading to the appearance of a split peak. This phenomenon has been reported in studies analyzing the crystalline structure of MWCNTs. Such splitting may also result from structural defects or variations in the stacking order within the MWCNTs, affecting the diffraction pattern. Understanding these features is crucial for characterizing the quality and structural integrity of MWCNTs, as they influence the material's mechanical properties.[56,57]

The functionalization of MWCNTs led to a reduction in peak intensity in the XRD pattern, indicating structural alterations in the nanotube framework. These changes can be attributed to the introduction of structural defects on the graphene walls caused by various functionalization methods, including acid treatments for COOH-MWCNTs, NH_2 modification, and silane coupling. The induced defects disrupt the orderly stacking of graphitic layers, diminishing the crystallinity of the nanotubes. This reduction in crystallinity is evident from the decreased intensity and slight broadening of the (002) peak, suggesting partial exfoliation or disorder in the carbon structure. Such structural modifications enhance the chemical reactivity of MWCNTs, improving their dispersion in polymer matrices and facilitating stronger interfacial interactions in nanocomposite applications.

The XRD pattern of the wear debris of the P-WMCNT and its derivative composite is shown in **Figure 10**; the typical characteristic peak of the (002) at 25° could not be seen in the wear debris. Instead, the broad peak appearing at 18.35° in XRD analysis likely corresponds to the disordered carbon structure or graphitic planes of MWCNTs. The appearance of a broad XRD peak at 18.35° suggests significant structural modifications in the MWCNTs, likely due to functionalization treatments. This broadening may indicate a transition to a more amorphous or disordered arrangement of the graphitic planes, as chemical treatments such as COOH functionalization, NH_2 modification, or silane coupling disrupt the orderly stacking of carbon layers. Functionalization, particularly through oxidation or surface treatments, introduces defects that broaden or shift peaks to lower angles, reflecting increased disorder and reduced crystallinity. According to Bragg's law,[58] the peak at 18.35° corresponds to a d-spacing of ≈4.83 Å (Cu Kα radiation $\lambda \approx 1.5418$ Å), which is notably larger than the typical 3.4 Å for well-ordered graphitic structures. This increased interlayer spacing further supports the conclusion that lubrication sliding creates significant disruptions in the structural integrity of the MWCNTs, diminishing their crystalline characteristics.

To further investigate the structural behavior of COOH-MWCNTs under varying applied loads, XRD analysis was conducted on wear debris generated at loads of 5 N, 10 N, and 15 N, while maintaining constant test conditions of 5 Hz frequency and a sliding distance of 400 m. The results shown in Figure 10b demonstrate a gradual transformation of the characteristic (002) peak at 25° into a broad disordered peak at 18°, indicating increased structural disorder. This suggests that as the applied load increases, the MWCNT structure becomes progressively more disordered, with a tendency to flatten and gradually break down. The opening of the graphitic carbon structure promotes the for-

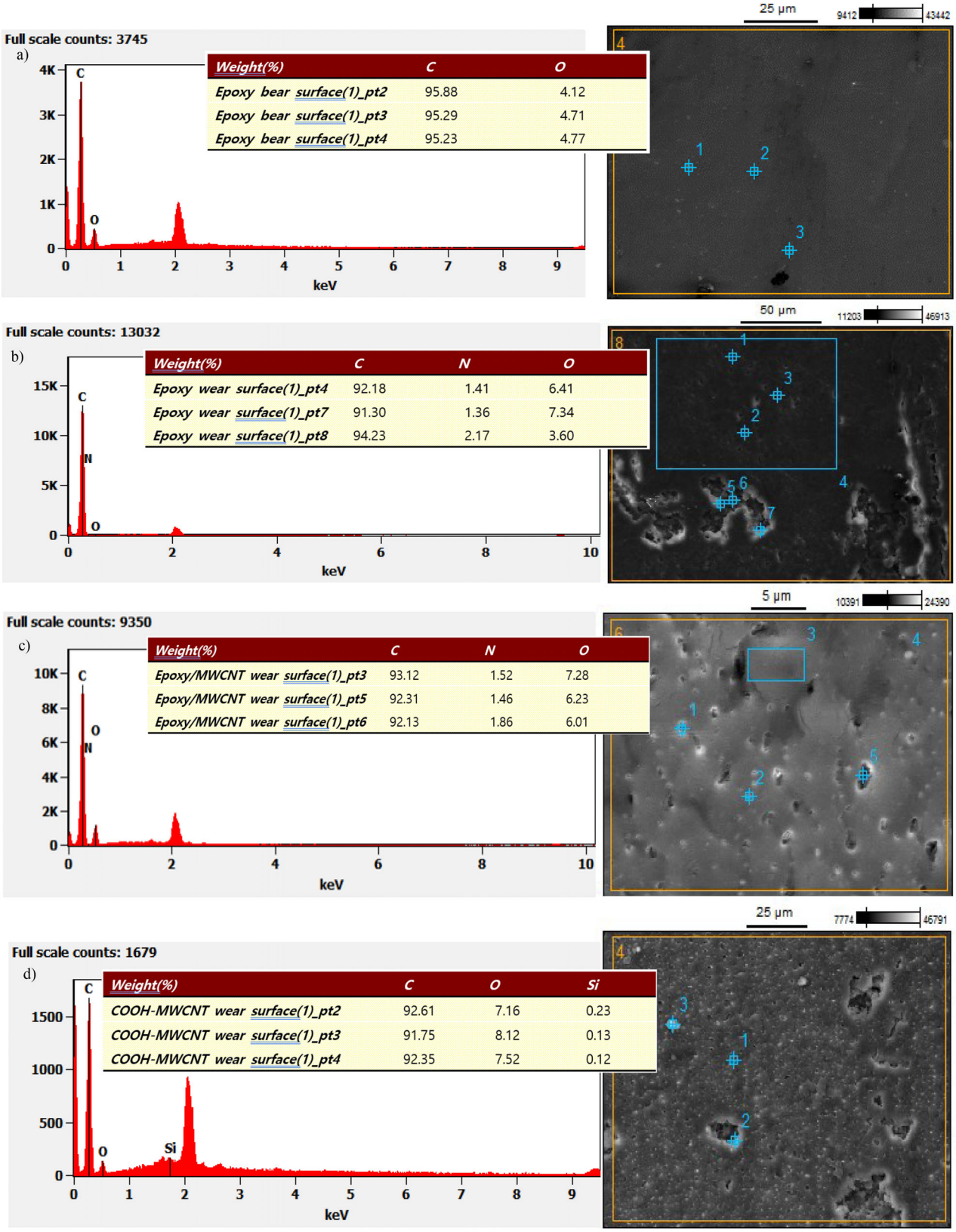

Figure 8. EDS elemental analysis of the wear track surface a) Neat epoxy surface; tested under 10N/5 Hz sliding condition after 400m b) epoxy: c) P-MWCNT/epoxy: d) COOH-MWCNT/epoxy: e) NH_2-MWCNT/Epoxy: f) Silane modified-MWCNT/Epoxy.

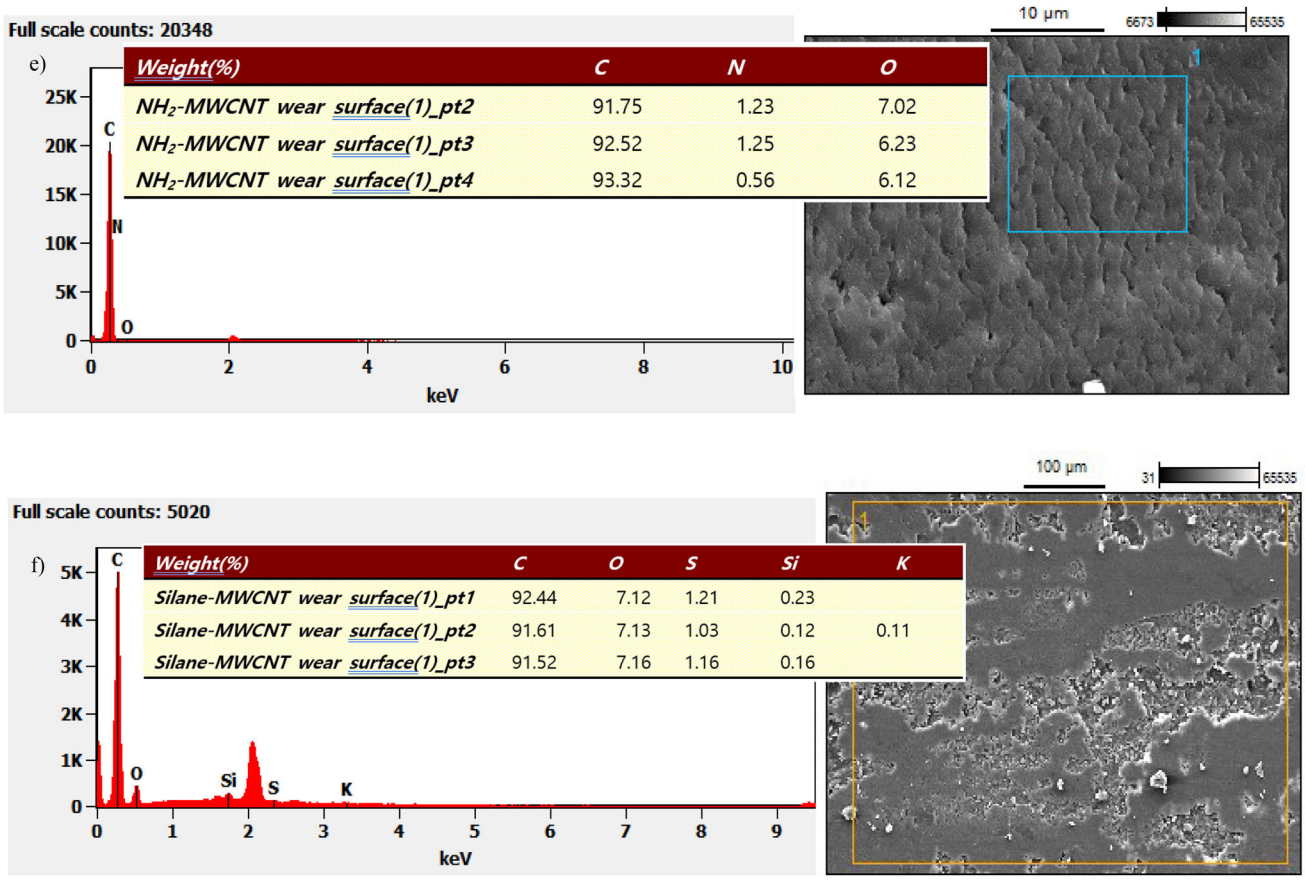

Figure 8. *Continued*

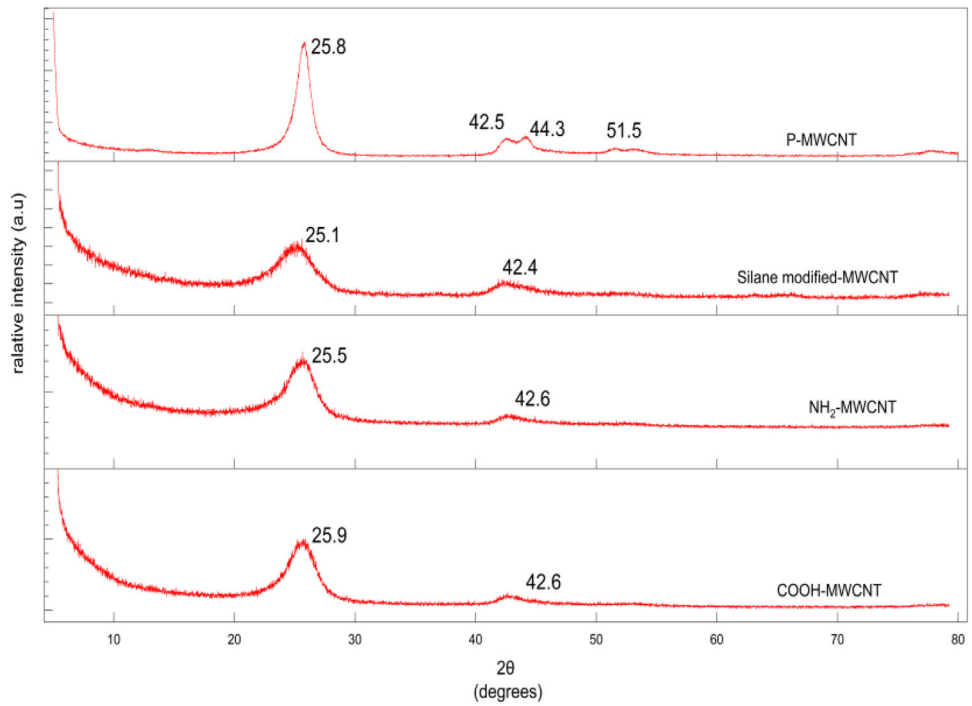

Figure 9. XRD pattern of P-MWCNTs and its derivatives.

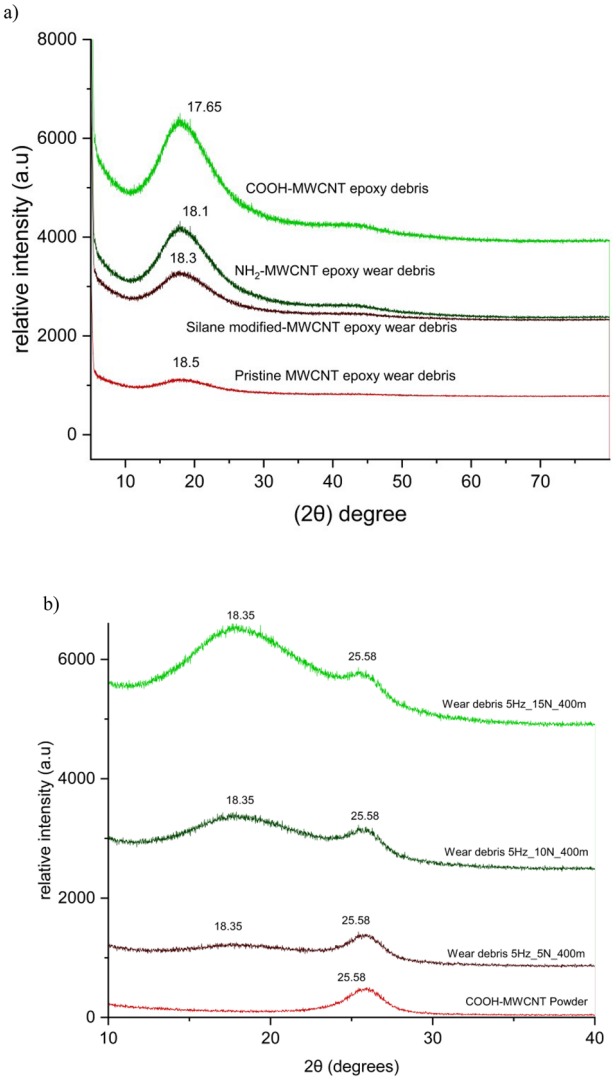

Figure 10. XRD patterns of wear debris collected after sliding tests. a) Wear debris from pristine MWCNTs and their derivative composite after sliding at 5 Hz, 10 N load, and a sliding distance of 400 m. b) Wear debris from COOH-functionalized MWCNT composites under increasing applied loads of 5 N, 10 N, and 15 N, compared with the XRD pattern of the original COOH-MWCNT powder.

mation of lubricating graphitic layers, effectively acting as a self-lubricating mechanism during sliding contact.

Figure 11 illustrates the wear surface morphology of COOH-MWCNT composites under varying magnifications. Figure 11a shows an overview of the composite's wear surface, highlighting a relatively smooth and compact structure. Figure 11b reveals regions where MWCNTs have flattened, forming a lubricative film-like layer that contributes to reduced friction during sliding. This structural transformation likely results from the applied load and sliding action, which cause the nanotubes to align and deform. Figure 11c presents fractured zones on the wear surface, where MWCNTs appear as fiber-like fragments protruding from the matrix. These exposed nanotube structures suggest mechanical breakage under higher loads, playing a crucial role in self-lubricating behavior by forming graphitic debris that aids in wear resistance.

3.7. TEM of Wear Surfaces

Figure 12 presents TEM images that provide critical insights into the structural deformation of MWCNTs during frictional interactions. Due to their high structural stability and strong sp^2 bonding, MWCNTs are inherently resistant to mechanical rupture. However, under tribological loading, MWCNTs actively migrate to the contact interface, where they participate in the self-lubrication mechanism. The TEM images illustrate the progressive rupture and unzipping of MWCNTs, which can lead to their transformation into graphitic structures under tribological conditions. As the applied load increases from 5N to 15N, this structural breakdown becomes more pronounced, facilitating the formation of graphitic tribofilms. These tribofilms contribute significantly to lubrication by reducing interfacial shear resistance. The findings suggest that increasing normal load accelerates the fragmentation of MWCNTs, promoting their structural transformation into graphitic layers, which enhance the self-lubricating properties of the composite.

The tribological behavior of MWCNTs is strongly influenced by their ability to form graphitic tribofilms, which act as a protective layer, reducing wear and friction. This transformation is largely driven by a combination of mechanical shear and friction-induced thermal effects at the contact interface. Additionally, the presence of reactive functional groups on the MWCNTs could further promote tribochemical interactions, enhancing the adhesion of graphitic layers to the worn surface. The continuous regeneration of these tribofilms suggests that MWCNT-reinforced composites could offer long-term durability in high-load applications, making them promising candidates for self-lubricating materials in advanced tribological systems.

As a summary, this research on epoxy composites reinforced with 0.3 wt.% MWCNTs (P-MWCNT, COOH-MWCNT, NH_2-MWCNT, and silane-modified MWCNT) demonstrates superior tribological and mechanical performance compared to many studies in the extended in the literature. Tribologically, COOH-MWCNTs exhibit the lowest COF (0.35 at 2 Hz, 0.38 at 5 Hz, 10N) and specific wear rate (SWR: 0.01–0.03 $\times 10^{-6}$ $mm^3\ N^{-1}{\cdot}m$ at 10N), outperforming neat epoxy (COF: 0.60–0.64, SWR: 0.27–0.40 $\times 10^{-6}$ $mm^3\ N^{-1}{\cdot}m^{-1}$). Compared to the literature, COOH-MWCNTs' COF is competitive with nanographene-filled epoxy (0.30,[59]) and graphite-filled epoxy (0.38,[60]), but higher than PTFE-filled epoxy (0.08–0.10,[61]). The SWR is notably lower than most studies, such as graphite-filled epoxy (1.5–4.0 $\times 10^{-5}$ $mm^3\ N^{-1}{\cdot}m^{-1}$,[62,64,60]) and even the typical MWCNT-epoxy range (1.0–5.0 $\times 10^{-6}$ $mm^3\ N^{-1}{\cdot}m^{-1}$,[64]), highlighting exceptional wear resistance. Compared to,[13] your -NH_2MWCNTs' SWR (0.04 $\times 10^{-6}$ $mm^3\ N^{-1}{\cdot}m^{-1}$ at 5 Hz, 10N) is far lower than their reported 0.953 $\times 10^{-4}$ gm min^{-1}, though units differ.

Mechanically, COOH-MWCNTs achieve a compressive strength of 90 MPa and Young's modulus of 1983.69 MPa, surpassing graphite-filled epoxy (tensile strength: 70 MPa,[63]) and nanographene-filled epoxy (flexural strength: 12% increase,[59]). The hardness of COOH-MWCNTs (≈88 Shore D) is higher than graphite-filled epoxy (80 Shore D,[62]), but slightly below

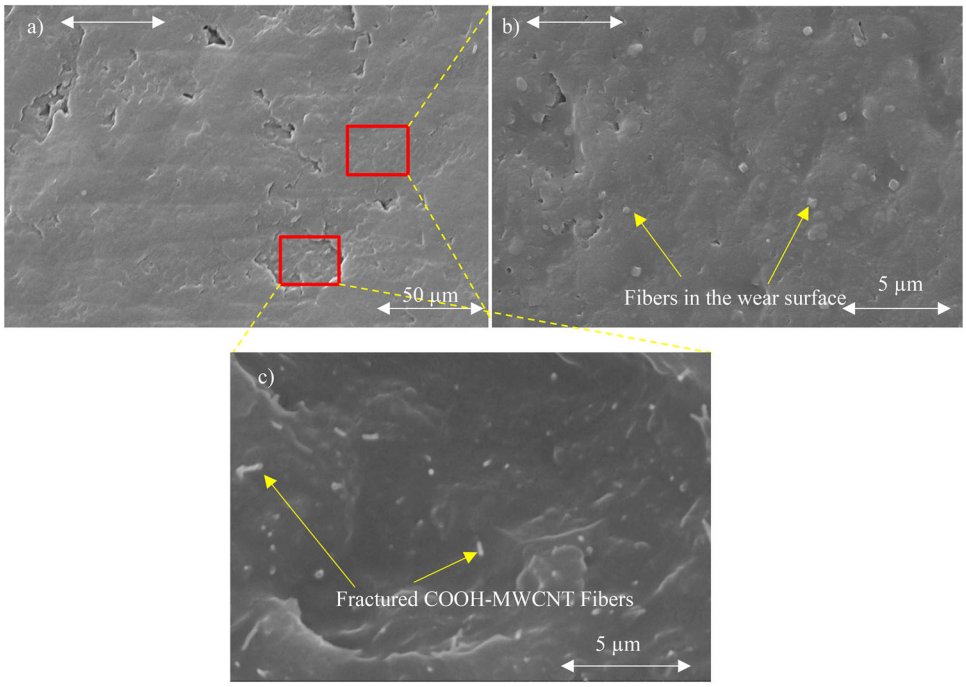

Figure 11. SEM images of the wear surface of COOH-MWCNT composites at different magnifications: a) Overall wear surface of the composite under lower magnification, b) Smooth wear surface, where the MWCNTs have flattened, and c) Fractured wear surface, revealing MWCNT fragments appearing as fiber-like structures.

nanographene-filled epoxy (90 Shore D,[59]). NH_2-MWCNTs' ductility (elongation: 10.46%) is notable, aligning with the need for balanced properties in applications like flexible seals.

The MoS_2/aligned MWCNT composite[65] shows a COF of 0.37 at 15N, closely matching COOH-MWCNTs at 5 Hz, 10N, but SWR is lower, indicating better wear resistance. Agglomeration above 0.3 wt.% in this study mirrors challenges in the literature,[13,62] emphasizing optimal filler content. The COOH-MWCNTs are ideal for automotive bushings and aerospace coatings, offering a superior balance of low friction, wear resistance, and mechanical robustness compared to many literature benchmarks.

The wear mechanism and structural transformation of MWCNTs, as analyzed through TEM and XRD, align well with the observed behavior of MWCNTs in the composite. Specifically, this study reveals that MWCNTs initially undergo shortening during wear, followed by flattening into a graphene-like lamella structure. This transformation reduces wear loss and contributes to a decrease in the friction coefficient consistent with mechanisms proposed in the literature. The formation of the graphene-like lamella acts as a protective layer, enhancing the tribological performance of the epoxy composite by minimizing surface damage and friction during sliding contact and having the good agreement with hypothetical mechanism illustrated in the literature.[31]

4. Conclusion

The integration of 0.3 wt.% COOH-MWCNTs into epoxy matrices, as explored in this study, aligns with the broader findings of the review on MWCNT-reinforced composites, demonstrating significant enhancements in tribological and mechanical properties. The review highlights that MWCNT-epoxy composites typically achieve a COF of 0.15–0.25 and wear rates of $1.0–5.0 \times 10^{-6}$ $mm^3\ N^{-1}{\cdot}m^{-1}$, attributed to CNTs' self-lubricating properties and high aspect ratio, which form protective tribofilms and enhance load distribution. Similarly, the COOH-MWCNT/epoxy composite exhibits a low COF (0.35 at 2 Hz, 0.37 at 15N) and an exceptional specific wear rate (SWR: $0.01–0.07 \times 10^{-6}$ $mm^3\ N^{-1}{\cdot}m^{-1}$), outperforming neat epoxy (COF: 0.60–0.66, SWR: $0.24–0.50 \times 10^{-6}$ $mm^3\ N^{-1}{\cdot}m^{-1}$). Mechanically, the composite's tensile strength (≈90 MPa), compressive strength (134 MPa), Young's modulus (1983.69 MPa), and hardness (≈88 Shore D) surpass neat epoxy (tensile strength: ≈45 MPa, compressive strength: 45.68 MPa, Young's modulus: 988.7446 MPa), with a 20–30% strength increase consistent with the review's findings. NH_2-MWCNTs offer balanced ductility (elongation: 10.46%), while silane-modified variants provide moderate strength (76 MPa) and ductility (elongation: 6.12%).

Practically, COOH-MWCNT composites are ideal for automotive suspension bushings, reducing friction (COF: 0.37) and wear (SWR: 0.07×10^{-6} $mm^3\ N^{-1}{\cdot}m^{-1}$) under 10N loads, ensuring durability. In aerospace, their wear resistance and hardness make them suitable for turbine blade coatings, while in industrial settings, they excel as sliding contact pads or conveyor rail coatings, minimizing maintenance. Additionally, their high strength and hardness support applications in protective coatings for cutting tools, molds, and biomedical joint implants, where NH_2-MWCNTs' ductility could enhance flexibility. However, limitations include agglomeration above 0.3 wt.%, which reduces performance, and a load threshold (15N), where COF and SWR in-

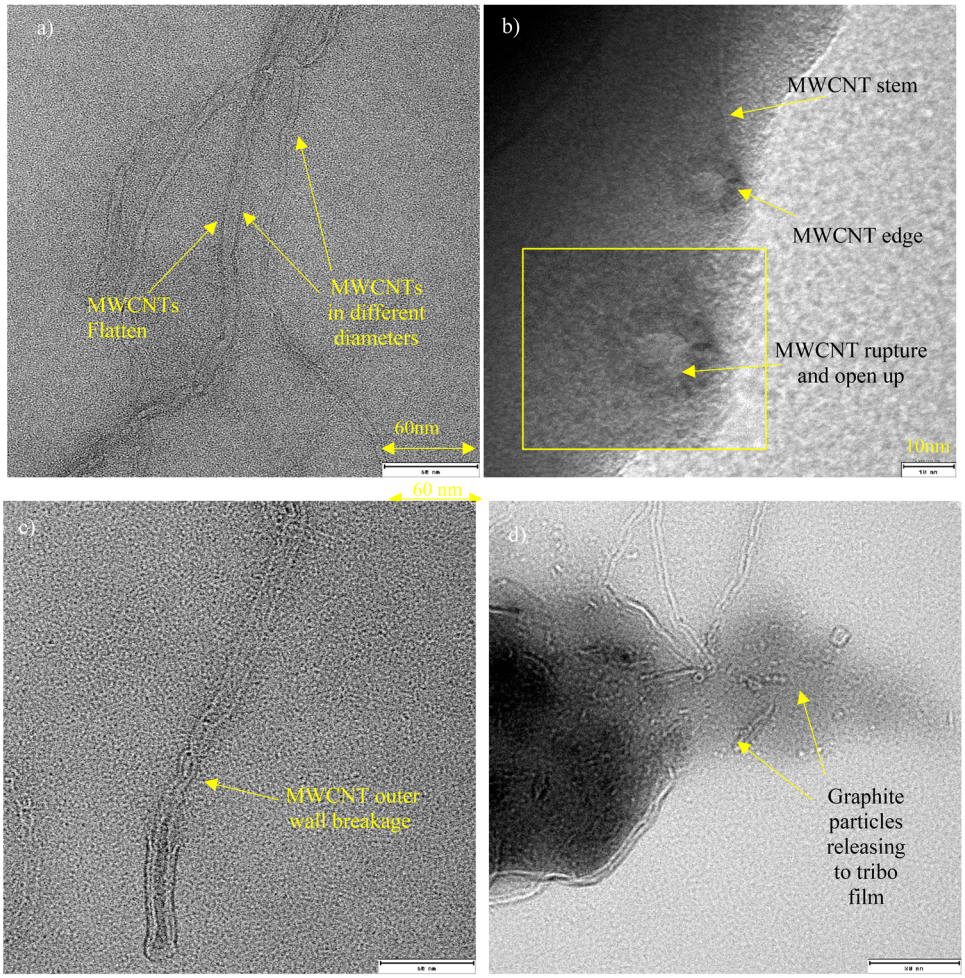

Figure 12. TEM images of the wear surface of COOH-functionalized MWCNT/composites wear debris at different loads: a) 5N_5Hz_400m; b,c) are 10N_5Hz_400m; d) 15N_5Hz_400m.

crease (0.56, 0.09×10^{-6} mm^3 $N^{-1} \cdot m^{-1}$), indicating sensitivity to high loads.

This study on COOH-MWCNT/epoxy composites highlights significant tribological and mechanical enhancements, yet several parameters remain unexplored, presenting opportunities for future research. The investigation did not consider the effects of environmental factors such as temperature, humidity, or corrosive conditions, which could influence the composite's performance in real-world applications like aerospace or automotive settings. Additionally, the study focused on a single filler concentration (0.3 wt.%), leaving the impact of varying MWCNT content (e.g., 0.1–1.0 wt.%) or hybrid fillers (e.g., combining MWCNTs with graphene or MoS_2) unaddressed. Future research should explore these variables to optimize load-bearing capacity and durability under extreme conditions. Investigating advanced dispersion techniques, such as high-shear mixing or chemical functionalization beyond COOH, NH_2, and silane groups, could further mitigate agglomeration issues observed above 0.3 wt.%. Moreover, evaluating the long-term wear behavior and fatigue resistance under cyclic loading will enhance the composite's applicability in dynamic environments, advancing the field of high-performance epoxy nanocomposites.

Acknowledgements

Open access publishing facilitated by Auckland University of Technology, as part of the Wiley - Auckland University of Technology agreement via the Council of Australian University Librarians.

Conflict of Interest

The authors declare no conflict of interest.

Data Availability Statement

The data that support the findings of this study are available from the corresponding author upon reasonable request.

Keywords

epoxy nanocomposites, multi-walled carbon nanotubes (MWCNT) functionalization, self-lubricating materials, tribological performance, wear mechanisms

Received: February 24, 2025
Revised: April 15, 2025
Published online:

[1] J. Ervina, M. Mariatti, S. Hamdan, *Procedia Chem.* **2016**, *19*, 897.
[2] I. Rafique, A. Kausar, B. Muhammad, *Polym.-Plast. Technol. Eng.* **2016**, *55*, 1653.
[3] A. Allaoui, S. Bai, H.-M. Cheng, J. Bai, *Compos. Sci. Technol.* **2002**, *62*, 1993.
[4] J. Cha, S. Jin, J. H. Shim, C. S. Park, H. J. Ryu, S. H. Hong, *Mater. Des.* **2016**, *95*, 1.
[5] S. Roy, R. S. Petrova, S. Mitra, *Nanotechnol. Rev.* **2018**, *7*, 475.
[6] E. Dervishi, Z. Li, Y. Xu, V. Saini, A. R. Biris, D. Lupu, A. S. Biris, *Part. Sci. Technol.* **2009**, *27*, 107.
[7] V. N. Popov, *Mater. Sci. Eng.: R: Rep.* **2004**, *43*, 61.
[8] A. Hameed, M. Islam, I. Ahmad, N. Mahmood, S. Saeed, H. Javed, *Polym. Compos.* **2015**, *36*, 1891.
[9] R. Konnola, K. Joseph, *RSC Adv.* **2016**, *6*, 23887.
[10] M. Ramesh, R. A. Ramnath, C. Deepa, in *Tribology of Polymer Composites: Characterization, Properties, and Applications*, Elsevier, Amsterdam, Netherlands **2021**, pp. 223–240.
[11] M. Venkatesan, K. Palanikumar, S. R. Boopathy, *Sci. Eng. Compos. Mater.* **2018**, *25*, 963.
[12] M. Mucha, A. Krzyzak, E. Kosicka, E. Coy, M. Kościński, T. Sterzyński, M. Sałaciński, *Materials* **2020**, *13*, 2696.
[13] L. J. Cui, H. Z. Geng, W. Y. Wang, L. T. Chen, J. Gao, *Carbon* **2013**, *54*, 277.
[14] R. A. Kurien, D. P. Selvaraj, M. Sekar, C. P. Koshy, K. M. Praveen, *Arab. J. Sci. Eng.* **2022**, *47*, 8059.
[15] M. Campo, A. Jiménez-Suárez, A. Ureña, *Wear* **2015**, 100.
[16] M. V. Hosur, T. Rahman, S. Brundidge-Young, S. Jeelani, *Composite Interface* **2010**, *17*, 197.
[17] J. Shen, W. Huang, L. Wu, Y. Hu, M. Ye, *Compos. Sci. Technol.* **2007**, *67*, 3041.
[18] M. I. Barrena, J. G. De Salazar, A. Soria, R. Cañas, *Appl. Surf. Sci.* **2014**, *289*, 124.
[19] P. Hiremath, R. Ranjan, V. DeSouza, R. Bhat, S. Patil, B. Maddodi, N. Naik, *J. Compos. Sci.* **2023**, *7*, 478.
[20] J. H. Lee, K. Y. Rhee, *J. Nanosci. Nanotechnol.* **2009**, *9*, 6948.
[21] Y. I. Wang, Q. Q. Ni, Y. Zhu, T. Natsuki, *Nano* **2014**, *9*, 1450011.
[22] P. C. Ma, J. K. Kim, B. Z. Tang, *Carbon* **2006**, *44*, 3232.
[23] M. H. Chung, W. H. Wang, L. M. Chen, C. W. Lee, P. F. Yang, Y. S. Liao, H. P. Lin, *Composites, Part A* **2015**, *78*, 1.
[24] G. Pincheira, C. Montalba, W. Gacitua, H. M. Montrieux, J. Lecomte-Beckers, M. F. Meléndrez, P. Flores, *Polym. Bull.* **2016**, *73*, 2287.
[25] M. Liu, D. Hou, L. Wu, *Mater. Today Commun.* **2022**, *33*, 104480.
[26] V. E. Ogbonna, A. P. I. Popoola, O. M. Popoola, S. O. Adeosun, *Polym.-Plast. Technol.* **2022**, *61*, 176.
[27] A. Imani, H. Zhang, M. Owais, J. Zhao, P. Chu, J. Yang, Z. Zhang, *Composites, Part A* **2018**, *107*, 607.
[28] O. Jacobs, W. Xu, B. Schädel, W. Wu, *Tribology Letters* **2006**, *23*, 65.
[29] K. Y. Eayal Awwad, B. F. Yousif, K. Fallahnezhad, K. Saleh, X. Zeng, *Friction* **2021**, *9*, 856.
[30] H. Wu, C. Liu, L. Cheng, Y. Yu, H. Zhao, L. Wang, *RSC Adv.* **2020**, *10*, 40148.
[31] M. M. Sakka, Z. Antar, K. Elleuch, J. F. Feller, *Friction* **2017**, *5*, 171.
[32] T. Zhou, X. Wang, X. H. Liu, J. Z. Lai, *eXPRESS Polym. Lett.* **2010**, *4*, 217.
[33] A. Bajpai, B. Wetzel, Tensile Testing of Epoxy-Based Thermoset System Prepared by Different Methods **2019**, pp 1–8, https://doi.org/10.20944/preprints201907.0143.v1.
[34] A. Rudawska, M. Frigione, *Polymers* **2022**, *14*, 2277.
[35] N. Chanshetti, A. Pol, *Int. Res. J. Eng. Technol* **2016**, *3*, 2395.
[36] K. Friedrich, *Adv. Ind. Eng. Polym. Res.* **2018**, *1*, 3.
[37] S. K. Sinha, B. J. Briscoe, *Polymer tribology*, World Scientific, Singapore **2009**.
[38] J. de Souza, I. Nascimento, S. Moreira, S. Cavalcanti, J. Medeiros, presented at *Pros. of the 21st Brazilian Congress of Mechanical Engineering*, Natal, Brazil, October **2011**.
[39] K. Yang, M. Gu, *Carbon* **2009**, *47*, 1723.
[40] H. Javed, M. Islam, N. Mahmood, A. Achour, A. Hameed, N. Khatri, *J. Polym. Eng.* **2016**, *36*, 53.
[41] O. Zabihi, M. Ahmadi, M. Naebe, *RSC Adv.* **2015**, *119*, 98692.
[42] J. H. Lee, K. Y. Rhee, J. H. Lee, *Appl. Surf. Sci.* **2010**, *256*, 7658.
[43] M. Premalatha, A. K. S. Jeevaraj, *Part. Sci. Technol.* **2018**, *36*, 523.
[44] B. Pratap Singh, V. Choudhary, S. Teotia, T. Kumar Gupta, V. Nand Singh, S. Rangnath Dhakate, R. Behari Mathur, *Adv. Mater. Lett.* **2015**, *6*, 104.
[45] T. Sun, H. Fan, Q. Zhuo, X. Liu, Z. Wu, *High Perform. Polym.* **2014**, *26*, 892.
[46] L. Gao, Q. Zhang, J. Guo, H. Li, J. Wu, X. Yang, G. Sui, *Thermochim. Acta* **2016**, *639*, 98.
[47] R. Shrivastava, K. K. Singh, *Compos. Interfaces* **2024**, *31*, 1133.
[48] S. Y. Wu, S. M. Yuen, C. C. M. Ma, C. L. Chiang, Y. L. Huang, H. H. Wu, M. H. Wei, *J. Appl. Polym. Sci.* **2010**, *115*, 3481.
[49] S. M. Yuen, C. C. M. Ma, C. L. Chiang, J. A. Chang, S. W. Huang, S. C. Chen, M. H. Wei, *Composites, Part A* **2007**, *38*, 2527.
[50] O. Eryilmaz, E. Sancak, *Polym. Compos.* **2021**, *42*, 6455.
[51] A. Kashyap, N. P. Singh, S. Arora, V. Singh, V. K. Gupta, *Bull. Mater. Sci.* **2020**, *43*, 1.
[52] L. Ramos-Galicia, J. López-Barroso, J. A. Rodríguez-González, C. Velasco-Santos, C. Rubio-González, A. L. Martínez-Hernández, in *Processing of Epoxy Composites Based on Carbon Nanomaterials–Epoxy Composites: Fabrication, Characterization and Applications*, Wiley, Hoboken, NJ, USA **2021**, pp. 125–175.
[53] Y. Zhou, F. Pervin, L. Lewis, S. Jeelani, *Mater. Sci. Eng., A* **2008**, *475*, 17.
[54] M. R. Saeb, F. Najafi, E. Bakhshandeh, H. A. Khonakdar, M. Mostafaiyan, F. Simon, E. Mäder, *Chem. Eng. J.* **2015**, *259*, 117.
[55] K. Yang, M. Gu, *Composites, Part A* **2010**, *41*, 215.
[56] O. V. Kharissova, B. I. Kharisov, *RSC Adv.* **2014**, *4*, 30807.
[57] S. M. Abdulkareem, R. M. Alsaffar, G. H. A. Razzaq, J. H. Mohammed, T. M. Awad, M. A. Alheety, S. Ghotekar, *J. Sol-Gel Sci. Technol.* **2024**, *111*, 979.
[58] M. P. Abdullah, S. A. Zulkepli, in AIP Conference Proceedings, AIP Publishing, NY, USA **2015**.
[59] H. Jagadeesh, P. Banakar, P. Sampathkumaran, R. R. N. Sailaja, J. K. Katiyar, *Tribol. Int.* **2024**, *192*, 109196.
[60] J. Smoleń, K. Stępień, M. Mikuśkiewicz, H. Myalska-Głowacka, M. Kozioł, M. Godzierz, J. Czakiert, *Materials* **2024**, *17*, 3054.
[61] K. Friedrich, Z. Zhang, A. K. Schlarb, *Compos. Sci. Technol.* **2005**, *65*, 2329.
[62] K. E. Awwad, *Tribology in Industry* **2024**, *46*, 298.
[63] M. M. Ibrahim, N. S. M. El-Tayeb, M. Shazly, M. M. El-Sayed Seleman, *Functional Composite Materials* **2024**, *5*, 2.
[64] F. Z. Zhang, X. B. Liu, C. M. Yang, G. D. Chen, Y. Meng, H. B. Zhou, S. H. Zhang, *Mater. Today* **2024**, *74*, 203.
[65] Z. Tong, J. Du, X. Li, Z. Liu, C. Yan, W. Lei, *Materials* **2024**, *17*, 4745.

